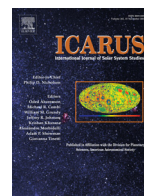




ELSEVIER

Contents lists available at ScienceDirect

Icarus

journal homepage: www.elsevier.com/locate/icarus

The age and the probable parent body of the daytime arietid meteor shower

Abedin Abedin*, Paul Wiegert, Petr Pokorný, Peter Brown

Department of Physics and Astronomy, The University of Western Ontario, London, Canada N6A 3K7, Canada

ARTICLE INFO

Article history:

Received 7 March 2016

Revised 10 August 2016

Accepted 14 August 2016

Available online xxx

Keywords:

Meteoroid stream

Formation

Age

Dynamics

ABSTRACT

The daytime Arietid meteor shower is active from mid-May to late June and is amongst the strongest of the annual meteor showers, comparable in activity and duration to the Perseids and the Geminids. Due to the daytime nature of the shower, the Arietids have mostly been constrained by radar studies. The Arietids exhibit a long-debated discrepancy in the semi-major axis and the eccentricity of meteoroid orbits as measured by radar and optical surveys. Radar studies yield systematically lower values for the semi-major axis and eccentricity, where the origin of these discrepancies remain unclear. The proposed parent bodies of the stream include comet 96P/Machholz [McIntosh, B.A., 1990. Comet P/Machholz and the Quadrantid meteor stream. *Icarus* 86, 894–299–304. doi:10.1016/0019-1035(90)90219-Y.] and more recently a member of the Marsden group of sun-skirting comets, P/1999 J6 [Sekanina, Z., Chodas, P.W., 2005. Origin of the Marsden and Kracht Groups of Sunskirting 922 Comets. I. Association with Comet 96P/Machholz and Its Interplanetary Complex. *ApJS* 923 161, 551–586. doi:10.1086/497374].

In this work, we present detailed numerical modelling of the daytime Arietid meteoroid stream, with the goal to identifying the parent body and constraining the age of the stream. We use observational data from an extensive survey of the Arietids by the Canadian Meteor Orbit Radar (CMOR), in the period of 2002–2013, and several optical observations by the SonotaCo meteor network and the Cameras for All-sky Meteor Surveillance (CAMS).

We find the most plausible scenario to be that the age and the formation mechanism of the Arietids is consistent with continuous cometary activity of 96P/Machholz over a time interval of $\approx 12,000$ years. The sun-skirting comet P/1999 J6 suggested by [Sekanina, Z., Chodas, P.W., 2005. Origin of the Marsden and Kracht Groups of Sunskirting 922 Comets. I. Association with Comet 96P/Machholz and Its Interplanetary Complex. *ApJS* 923 161, 551–586. doi:10.1086/497374.] may contribute to the shower, but the comet break up prior to 950 CE they propose does not reproduce all the characteristics of the observed shower.

© 2016 Elsevier Inc. All rights reserved.

1. Introduction

The daytime Arietids meteor shower, designated as “00171 ARI” by the International Astronomical Union Meteor Data Center (IAU MDC) <http://www.ta3.sk/IAUC22DB/MDC2007/>, is amongst the strongest annual showers, comparable in activity and duration to the major night-time meteor showers such as the Perseids and Geminids (Aspinall and Hawkins, 1951; Campbell-Brown, 2004). Despite its prominence, the shower has only recently begun to be characterized, as the radiant is close to the Sun and hence the shower is mainly accessible via radar techniques. A daytime shower is defined by the International Astronomical Union (IAU) as having a radiant position within 30° from the Sun at maximum

activity, thus limiting video observations to one hour before sunrise or one hour after sunset. The daytime Arietids are observed annually from mid-May to late June where the core of the activity profile is located between solar longitudes $73.5^\circ < \lambda_\odot < 84.5^\circ$, with a broad 4-day maximum centered at $\lambda_\odot = 80.5^\circ$ (Bruzzone et al., 2015). The duration and the broad maximum of the core of the stream implies an old age, perhaps of order of a few millennia. Despite the proximity of the radiant to Sun, its detectability is not strictly limited to radar techniques. There have been a handful of Arietids detected by TV techniques in the hours before dawn (Fujiwara et al., 2004; Jenniskens et al., 2016; SonotaCo, 2009).

The parent of the Arietids remains uncertain, although the stream has previously been linked to comet 96P/Machholz (Babadzhanov and Obruchov, 1992; Jones and Jones, 1993; McIntosh, 1990) and more recently to the Marsden group of sun-skirting comets (Jenniskens et al., 2012; Ohtsuka et al., 2003; Sekanina and Chodas, 2005). Interestingly, there are significant

* Corresponding author.

E-mail address: aabedin@uwo.ca (A. Abedin).

discrepancies in the semi-major axis and eccentricity of Arietid meteors as measured by radar and video techniques. Radar measures systematically lower values for the semi-major axis, with values as low as 1.6 AU, while optical semi-major axis values typically lie between 2–3.5 AU. If these differences are real, this suggests a strong mass-dependent semi-major axis sorting of the stream, a feature which formation models must explain.

Generally, radar observations of meteors are less precise than those accomplished by video techniques (Hawkes, 1993, 2002; McKinley, 1961). The largest uncertainty is typically in the geocentric velocity of the meteoroids, which translates into an uncertainty in the semi-major axis of the orbit. Although modern meteor radar detections have significantly improved in precision over the past few decades, (see e.g., Baggaley et al., 1994; Jones et al., 2005), the puzzle of the large difference in the semi-major axis of the Arietids, measured by different techniques, namely radar and TV, remains unsolved. Jenniskens et al. (2012) suggested that the discrepancy in the semi-major axes, obtained by radar measurements may be due to the improper correction for the deceleration of the meteors in the Earth's atmosphere.

In the period 2002 to 2013, the Canadian Meteor Orbit Radar (CMOR) carried out an extensive survey of the daytime Arietids, where more than 2×10^4 meteor orbits with representative masses of 8×10^{-8} kg and sizes ≈ 400 μm , were measured (Bruzzone et al., 2015). This allowed for the observed characteristics of the Arietids to be relatively well constrained. In particular, that study focused on attempting to provide a best estimate of the speeds of the Arietids. Despite their work, the result remains that CMOR radar-derived speeds are noticeably lower than optical measurements, consistent with lower speeds measured in earlier radar surveys (Bruzzone et al., 2015).

Based on that decadal survey, the Arietids were found to move on orbits with a mean perihelion distance in the order of 15 solar radii (≈ 0.075 AU). Optical techniques yield slightly lower perihelion distance ($q \approx 13 R_{\odot}$). The orbit of the often cited parent comet 96P has a current perihelion distance of 0.12 AU $\approx 25 R_{\odot}$ but undergoes a Kozai type oscillation (Bailey et al., 1992), where the perihelion distance q of the comet swings between the extremely low value of ≈ 0.05 AU to about 1 AU, with a period of ≈ 4500 years.

The similar evolutionary behavior of the orbits of the Arietids led McIntosh (1990) to suggest a sibling relationship between the daytime Arietids, comet 96P/Machholz and the Southern Delta Aquariids based on the similar secular evolution of their orbits. Although the present perihelion distance of the orbit of 96P is much greater than that of the Arietids, both the lines of apses of the Arietids and 96P have similar orientation in the space of the ecliptic longitude and latitude (L_{π} , B_{π}), suggesting that they may be related but are in a different phase of the Kozai cycle. Babadzhanov and Obrubov (1992); 1993) showed that comet 96P, in addition to the daytime Arietids, can produce 8 meteor showers in total (among them the Quadrantids, Ursids, Carinids, α -Cetids, κ -Velids, Northern and Southern δ -Aquariids) within one precession cycle of the comet. Jones and Jones (1993) carried out numerical simulations to study the formation of the Quadrantid meteoroid stream and confirmed the results from previous studies that meteoroids ejected from 96P/Machholz can produce the daytime Arietids, as well as some of the streams proposed by Babadzhanov and Obrubov (1992, 1993). They argued that 96P/Machholz was captured into a 2:1 mean motion resonance with Jupiter some 2200 years ago, and predicted that some of the resulting meteoroid streams must exhibit a bimodal activity distribution due to the resonance.

Comet 96P/Machholz has been classified as a Jupiter Family Comet (JFC) (<http://ssd.jpl.nasa.gov/sbdb.cgi>) with a Tisserand parameter with respect to Jupiter of $T_J = 1.942$, a value typical for

Halley-type Comets (HTCs) (see e.g., Carusi et al., 1987). The Tisserand parameter is a quasi-constant arising from the “restricted 3-body problem” (e.g., Murray and Dermott, 2000) and is not strictly conserved for the N-body problem (where $N > 3$). Thus, it is difficult to classify 96P as originating from HTCs or not.

Another interesting feature of 96P is the reported unusual chemistry of the comet (Langland-Shula and Smith, 2007; Schleicher, 2008). During post-perihelion photometric and spectroscopic observations of 96P, it was noted that the comet exhibits anomalously low C_2 , C_3 and CN production, relative to NH, an observation confirmed for only a few other comets (A'Hearn et al., 1995). Schleicher (2008) argued that may be an indicator for an extrasolar origin of 96P, or abnormal thermal alteration of its chemistry via unclear processes. This features of 96P/Machholz render the origin of the daytime Arietids extremely interesting, if the later originated from 96P.

The extremely low perihelion distance, of the mean orbit of the daytime Arietids, led Sekanina and Chodas (2005) to suggested that the stream is perhaps more closely related to the Marsden and Kracht's group of sunskirting comets, rather than to comet 96P/Machholz (see also Ohtsuka et al., 2003; Jenniskens et al., 2012). The tendency of most sun-skirting (Marsden and Kracht) and sun-grazing (Meyer and Kreutz) groups of comets to arrive at perihelion as doublets and triplets suggests that the Meyer and Kreutz sunskirters, along with P/1999 J6 and 96P/Machholz, may have originated from a fragmentation of a single large body, prior to 950 AD (Sekanina and Chodas, 2005). The authors referred to that large parent as the first generation fragment, and deduced a few likely break-up epochs - 150 AD, 350 AD, 500 AD, 700 AD and 950 AD.

In the process of testing the parent-child relationship of a meteoroid stream and a comet or an asteroid, it is customary to assume a given parent body, and then to model the resulting meteoroid stream numerically. However, the assumption that the Arietids are related to the Marsden group of comets renders it impractical to test child-parent relationships with each individual member of the group. Instead we will consider the most notable member, among the ≈ 35 comets in the group, namely comet P/1999 J6 (Sekanina and Chodas, 2005), and test it as a potential parent of the Arietids. The choice of P/1999 J6 as a potential parent of the Arietids is further motivated by the fact that P/1999 J6 is the brightest and has the best constrained orbit (with data arc-span of ≈ 11 years <http://ssd.jpl.nasa.gov/sbdb.cgi>) than any other member of the Marsden group and was suggested as the immediate parent of the Arietids by Sekanina and Chodas (2005).

In summary, previous authors have suggested that either comet 96P/Machholz or the Marsden group of sunskirters are the most probable parents of the daytime Arietid meteor shower, but there has not yet been a detailed dynamical study dedicated to understanding the formation and evolution of the daytime Arietid meteoroid stream. Such a study must match and explain the observed characteristics of the stream, particularly the orbital characteristics, activity profile and radiant. This work is a first attempt to fill this gap. The goal of this study is to understand the “child-parent” relationship between the daytime Arietids and comet 96P/Machholz and/or P/1999 J6, based on the observed (radar and video) characteristics of the shower and to provide a best estimate for the age of the stream.

2. Observations

The earliest radar detections of the Arietids were made by Clegg et al. (1947), who reported increased meteor activity from a radiant near η -Aquarii, in 1946. It was not until 1949 when Aspinall et al. (1949) correctly determined the radiant position.

Davies and Greenhow (1951) were the first to use radar to measure the in-atmosphere speeds of the Arietids. They found a value of 38.5 km.s^{-1} based on observations from 1949 and 37.6 km.s^{-1} using observations from 1950, leading to the determination of the first set of orbital elements for the stream (Almond, 1951). For an extensive historical overview of radar observations of the Arietids, the reader is referred to Bruzzone et al. (2015).

Contemporary radar observations of meteor showers, e.g. Advanced Meteor Orbit Radar (AMOR Baggaley et al., 1994) and Canadian Meteor Orbit Radar (CMOR Jones et al., 2005) have significantly improved the number and quality of the measured meteoroid stream orbits. The daytime Arietids have been extensively studied by CMOR, where in the period 2002–2013 more than 2×10^4 Arietids, with representative masses of $8 \times 10^{-8} \text{ kg}$, were recorded (Bruzzone et al., 2015). It is notable that meteors at these sizes are difficult to observe optically, due to their small masses. However, a handful of optical observations of larger Arietids do exist (see e.g., Fujiwara et al., 2004; SonotaCo, 2009; Jenniskens et al., 2016) despite the proximity of the radiant position to the Sun. Our modeling of the Arietids will mainly use the radiant and activity profile of the stream reported in the decadal survey of the shower by CMOR (Bruzzone et al., 2015). We augment these data with 14 TV Arietids recorded by the SonotaCo network (SonotaCo, 2009) and 31 video events by the Cameras for All-sky Meteor Surveillance (CAMS), detected between 2011 and 2012 (Jenniskens et al., 2016).

It is widely accepted that individually measured photographic and TV meteoroid orbits yield more accurate pre-atmospheric speed (and hence orbital elements) than radar techniques, (e.g., Hawkes, 1993, 2002). However, the large number of individually recorded Arietid orbits by CMOR provide a solid statistical constraint of the observed characteristics of the Arietids in the hundreds of μm size range, particularly radiant location and activity profile.

In the literature, there are large differences in the pre-atmospheric speeds of individual Arietids reported by radar as compared to optical techniques (see e.g., Jenniskens et al., 2011, 2016; Bruzzone et al., 2015). In particular, the radar measurements yield systematically lower pre-atmospheric speeds for the stream, as compared to optical observations. This difference reaches values as high as 2 km/s (see Table 1 and Table 2 of Bruzzone et al. (2015)), resulting in a difference in the calculated semi-major axes of the meteoroids of more than 1 AU (see Fig. 18 of Bruzzone et al. (2015)). Fig. 1 shows the orbits of the mean Arietids stream as measured by CMOR and CAMS, along with the orbits of the potential parents, considered in this work.

It is not clear whether this difference in the speeds as measured by optical and radar techniques implies a mass segregation of the meteoroids or to systematic technique-specific errors. The best estimate after careful comparison to ablation modeling of the mean pre-atmospheric geocentric speed of the Arietids by CMOR (Bruzzone et al., 2015) yields, $V_g = 38.9 \pm 0.7 \text{ km.s}^{-1}$, where the same quantity obtained from TV observations of 14 Arietids is $V_g = 40.55 \pm 0.47 \text{ km.s}^{-1}$ (SonotaCo, 2009) and $V_g = 40.70 \pm 1.59 \text{ km.s}^{-1}$, based on 31 video events (Jenniskens et al., 2012). The resulting semi-major axis of the mean Arietids with corresponding one standard deviation, based on the CMOR is $a = 1.7 \pm 0.2 \text{ AU}$ (Bruzzone et al., 2015), $a = 2.34 \pm 0.6 \text{ AU}$ based on 14 TV Arietids (SonotaCo, 2009) and $a = 2.768 \pm 0.812 \text{ AU}$ according to Jenniskens et al. (2016) as measured by CAMS (for details and comparison between the other orbital elements, see Table 2 of Bruzzone et al. (2015)). This difference in the speeds and semi-major axis is comparable to the scatter of the different measurement techniques. That logically leads to the question whether these differences can be associated to the modeled deceleration of the meteoroids in the Earth's atmosphere or are arti-

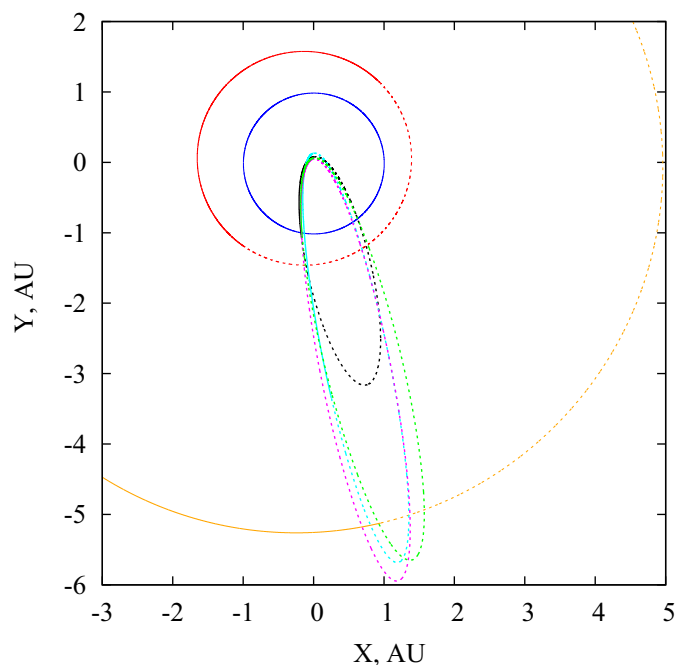


Fig. 1. The orbits of 1999 J6 (magenta), 96P (cyan) and the mean of the daytime Arietids⁽¹⁾ (black) from CMOR and daytime Arietids⁽²⁾ (green) from CAMS, as seen from above the ecliptic plane. The portion of the orbits below the ecliptic are presented with a dashed line. The orbits of the Earth (blue), Mars (red), and Jupiter (orange) are also shown. ⁽¹⁾The mean orbital elements of the Arietids, based on radar survey, are taken from Bruzzone et al. (2015). ⁽²⁾The mean orbital elements of the Arietids, based on optical survey, are taken from Jenniskens et al. (2016). (For interpretation of the references to colour in this figure legend, the reader is referred to the web version of this article.)

cial due to the large scatter in the optical surveys. Smaller meteoroids (hundreds of μm) are subject to greater deceleration in the Earth's atmosphere, as compared to the millimeter or centimeter size particles that are detected optically. Jenniskens et al. (2012) attributed the differences in the pre-atmospheric speeds as measured by CMOR and optical techniques (e.g. CAMS) to an improper account for the deceleration of the Arietids, where the deceleration corrections employed are mean values from observations of other meteor showers with known speeds.

This difference may also be due to mass segregation of meteoroids along the mean orbit of the Arietids. Mass segregation has been demonstrated in the dynamical modelling of many streams (e.g., Vaubaillon et al., 2006; Jenniskens and Vaubaillon, 2007; 2010; Neslušan and Hajduková, 2014; Jakubík and Neslušan, 2015). In this case, the inconsistency in the speeds and orbital elements is one of appearance only. The size and mass of the meteoroids affect the dynamics mainly through the non-gravitational forces from the Sun, namely solar radiation pressure and Poynting–Robertson drag (see e.g., Burns et al., 1979), where these forces are more significant on smaller particles. While the solar radiation pressure acts to weaken the solar gravity, the Poynting–Robertson drag causes the angular momentum of the meteoroids to decrease, resulting in a decrease of their semi-major axis and eccentricity. Thus, it is expected that the semi-major axes of smaller meteoroids will decrease over time, resulting in a natural separation between small and large particles purely due to radiation effects.

In our simulations of the daytime Arietids, in addition to constraining the most likely parent and age of the stream, we attempt to address the question as to whether the observed differences in the orbital elements as deduced by radar and TV observations are real or an instrumental artifact.

3. Numerical simulations

3.1. Stage I - Backward integrations of potential stream parent bodies

We first integrate the orbits of both proposed parents 96P/Machholz and P/1999 J6, backwards in time along with 10^4 clones for each parent. These integrations provide us with a starting point from which forward modelling of meteoroid stream production by the proposed parents can proceed. The clones are sampled from the six-dimensional orbital phase space using the covariance between the orbital elements, following an approach similar to [Brasser and Wiegert \(2008\)](#). The orbital elements of a given clone y_i can be written in the form:

$$y_i = y_o + X_{ik} \Lambda_{kj} \xi_j, \quad (1)$$

where y_o is a 6×1 column vector of the nominal orbital elements of the comet, X_{ik} is 6×6 matrix with columns equal to the eigenvectors of the covariance matrix, Λ_{kj} is a 6×6 diagonal matrix with elements corresponding to the eigenvalues of the eigenvectors, ξ_j is a column vector of random numbers drawn from a Gaussian distribution with mean value $\mu = 0$ and standard deviation $\sigma = 1$. The osculating orbital elements as well as the covariance matrix for the orbital elements of the comets were taken from the NASA's JPL Horizon system: <http://ssd.jpl.nasa.gov/sbdb.cgi>. During the backward integrations, we accounted for the gravitational perturbations from all the planets and also allowed for their mutual interactions, where the Earth and the Moon were taken together, i.e. their barycenter. We used the JPL's DE 405 integrated planetary ephemeris file (<ftp://ssd.jpl.nasa.gov/pub/eph/planets/ascii/>) to generate the state vectors of the planets, for a given epoch for which the osculation elements of either of the comets are available.

The clones in our simulations were considered as test particles, i.e. their mutual interaction and collisions were neglected. Considering the behavior of the clones and not solely the nominal orbit provides a measure of the confidence we can ascribe to the parent's past history. If many of the clones behave in a consistent way, we can assert that the parent did as well, while if the clones disperse, our own confidence in the past dynamical evolution of the parent disperses with them.

Finally, for both forward and backward simulations we used the Chambers' hybrid symplectic scheme ([Chambers, 1999](#)) which is a good compromise between accuracy and speed. Throughout the simulations, we maintained a constant time step which was different for both parents due to their different perihelion distances. However, prior to the main integrations several tests were performed in order to choose optimal time steps for both parent – being small enough so that it accurately describes the motion near the Sun, but also large enough to mitigate against the accumulation of numerical errors.

3.2. Parent candidate # 1: P/1999 J6

Numerical integrations of high-eccentricity orbits require careful choice of time step so that the motion around perihelion is well-sampled. Because of the extremely low perihelion distance of P/1999 J6 ($q \approx 10R_{\odot}$), before the main backward integrations, we tested various integration time steps, ranging from 1 to 12 hours. We found that a time step of 4 hours is a good compromise between integration speed and accuracy: that time step was used throughout the backward integrations of P/1999 J6. In addition to Newtonian gravity, we also accounted for the primary general relativistic effects (through the post-Newtonian approximation), despite the fact that 1999 J6 spends only a short time in the vicinity of the Sun. The equations of motion of all planets, P/1999 J6, and its clones, were integrated backwards in time for 2000 years, i.e. until 0 CE. This time scale was chosen, in conformance with the

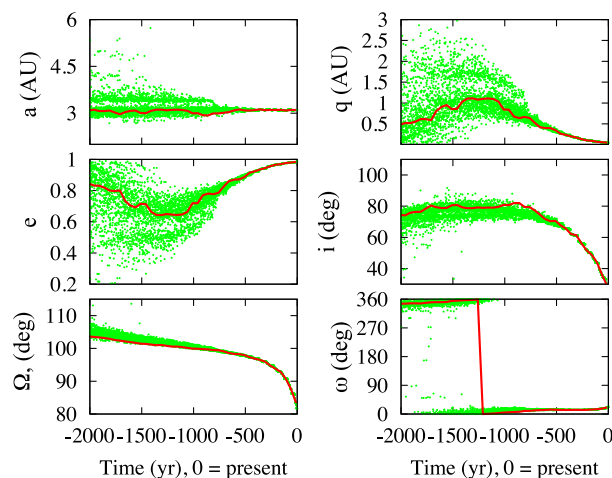


Fig. 2. Backward evolution of the nominal orbital elements of comet P/1999 J6 (red), along with 10^4 clones (green), over 2000 years. (For interpretation of the references to colour in this figure legend, the reader is referred to the web version of this article.)

conjecture that the P/1999 J6 broke up from a larger progenitor, between 100 CE and 950 CE ([Sekanina and Chodas, 2005](#)). We emphasize that, although P/1999 J6 arguably separated from a larger progenitor via fragmentation (thermal or tidal disruption), we assume here that the meteoroid ejection mechanism will be standard cometary sublimation. [Sekanina \(1977\); 1978](#) showed that the separation velocities between fragments of split comets is of the order of a few m/s, a few orders of magnitude less than the ejection speeds of meteoroids from the surface of a low-perihelion comet. Thus, we do not expect that a possible splitting of P/1999 J6 would result in a broader stream than that due to the normal outgassing of a comet.

During the backward integrations, we found that the orbit of P/1999 J6 quickly becomes chaotic, over a time scale of approximately 500 years, which is evidenced by the dispersal in the orbital elements displayed in [Fig. 2](#). This stochastic behavior imposes limits as to how reliably one can know the past osculating orbital elements of P/1999 J6, which are used here for meteoroid ejection and integration of their orbits forward in time. However, a careful selection of sets of orbital elements of P/1999 J6 (or clones), at a given epoch in the chaotic region, may still be used for meteoroid ejection. The key point is to select clones which are located close to the nominal orbit, and use them as the virtual meteoroid parent, when integrated forward in time. Because the scattering of the clones arises primarily in this case, from planetary encounters, parent-clones which are located far from the nominal orbit cannot match the timing, spread of the activity profile and radiant location of the current Arietids. Such an occurrence would require that all or nearly all of the meteoroids they eject suffer planetary encounters that place them on the present Arietid orbit, which cannot happen in practice due to the stochastic nature of planetary encounters. In this manner, we select clones which could with reasonable probability reproduce the daytime Arietids as we see them today. Though we can push a certain extent into the chaotic zone, we do not attempt to go further back than 2000 years.

3.3. Parent candidate # 2: 96P/Machholz

As a possible parent, the orbit of comet 96P was integrated backwards in time along with 10^4 clones until 50,000 BC. The length of the integration was chosen somewhat arbitrarily, mainly because of a lack of a priori knowledge as to the age of Arietids and secondly we aimed to obtain a broader picture as to the overall backward evolution of the orbit of comet 96P. Moreover, the

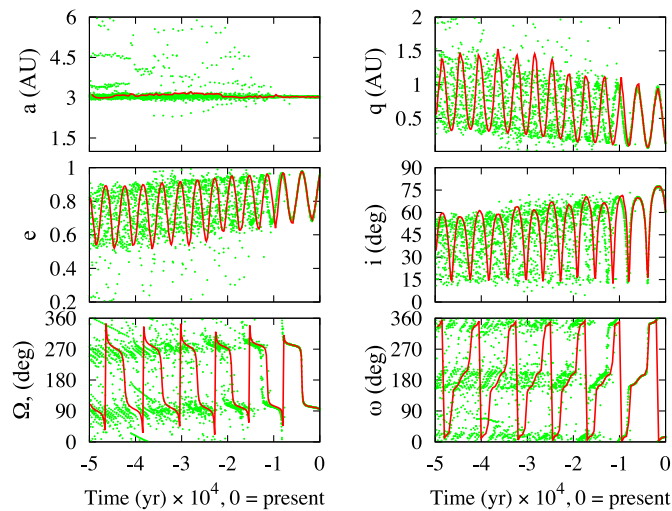


Fig. 3. Backward evolution of the nominal orbital elements of comet 96P/Machholz (red), along with 10^4 clones (green), over 5×10^4 years. (For interpretation of the references to colour in this figure legend, the reader is referred to the web version of this article.)

long duration of the shower's activity (more than a month) indicates that it is likely old if it formed by standard cometary activity. Although, our backward integrations span until 50,000 BC, we will only consider meteoroid ejections, starting circa 10000 BC. The reason is that it is although the dynamical lifetime of JFCs is $\sim 4.5 \times 10^4$ (e.g., Levison and Duncan, 1994), the physical lifetimes of these comets have a median value $\sim 1.2 \times 10^4$ years (e.g., Levison and Duncan, 1997). Thus, it is unlikely that 96P could have survived on such an orbit over 50 millennia. Furthermore, the epoch of 10,000 BC is also motivated by the chaotic behavior of the 96P's orbit during backward integrations beyond 7500 BC. In spite of 10,000 BC being in the chaotic region (defined by the backward integrations), a careful selection of clones (Section 3.4.3 and Fig. 4) used for meteoroid ejection could perhaps still provide some information as to the approximate "true" evolution of 96P's orbit.

As with P/1999 J6, we utilized the hybrid symplectic integrator, the only difference being that a larger time step of 12 h was used. Time steps between 2–24 h were tested beforehand in order to determine an optimal value between the integration speed and accuracy. For each test time step, the orbit of 96P was integrated backwards in time for 7500 years (or before the orbit becomes chaotic) and then forward in time until the present. The next step was a comparison of the differences between starting and end orbital elements for each time step. We chose to use a time step of 12 h, because it was the longest time step that yielded similar results over 7500 years when compared to simulations with shorter time steps.

Furthermore, the same assumptions for the planets accounted for, non-gravitational effects etc., were used as those in the case of the backward integrations of P/1999 J6 (see Section 3.2). The orbit of 96P evolves smoothly over 7500 years into the past before planetary encounters begin to disperse the clones (Fig. 3). Moreover, the evolution of the orbit of 96P is dominated by the Kozai oscillation (Kinoshita and Nakai, 1999; Kozai, 1962), which manifests itself in a distinct correlation between the eccentricity (e), inclination (i) and argument of perihelion (ω) of the orbit, a condition often seen in sun-grazing comets (Bailey et al., 1992).

3.4. Stage II - meteoroid ejection and forward integrations

The formation of meteoroid streams is relatively well understood. In the classical meteoroid formation model (Whipple, 1950;

Table 1

Various meteoroid ejection scenarios from P/1999 J6. For all cases, it is assumed a constant continuous cometary activity between the onset time and the present. The meteoroids are released from each individual clone at every fifth perihelion return until the present. Assuming, a period of $P = 5.3$ years for P/1999 J6, meteoroid release takes place every ≈ 26.5 years.

Case No	Met. ejection onset	Num. of every fifth perihelion returns of P/1999 J6 N_p	Num. of met. ejected at every fifth perihelion N_e	Total number of simulated particles $N_{tot} = N_p \times N_e$
1	150 CE	70	250×10 clones	$\approx 1.8 \times 10^5$
2	350 CE	62	250×10 clones	$\approx 1.6 \times 10^5$
3	500 CE	52	250×10 clones	$\approx 1.3 \times 10^5$
4	700 CE	45	250×10 clones	$\approx 1.1 \times 10^5$
5	950 CE	37	250×10 clones	$\approx 9.2 \times 10^4$

1951), meteoroids are released from the surface of the comet due to sublimating gas. Thus, meteoroids move with a slightly different velocity than the comet which results in, among other things, a small change in the orbital energy and semi-major axis of the particles. As this change in a also produces a change in the orbital period, meteoroids will tend to disperse along the orbit of the comet, resulting in a closed stream of meteoroids (e.g. Williams, 1992). Furthermore, the solar radiation pressure, acting on the meteoroids, will counteract the gravitational pull by the Sun, effectively weakening the Solar gravity. This in turn will cause the semi-major axis of meteoroids to increase, resulting in a mass segregation along the orbit (e.g. Kresak, 1976). The dynamical evolution of the stream will further be affected by planetary perturbations and eventually, if at some point in time the stream crosses the Earth's orbit, it may produce a meteor shower. In this section, we describe the meteoroid ejection model and the forward integrations of the resulting particles, with an aim to investigate the synthetic meteoroid streams of comets P/1999 J6 and 96P.

3.4.1. Meteoroid ejection modeling

Without a priori knowledge of the exact chemical composition and physical structure of the meteoroids, producing the daytime Arietids, we decided to model the meteoroids as spherical particles of density 2.5×10^3 kg/m³. The latter is somewhat a mean value based on recent studies of meteoroid densities (e.g., Babadzhanyan and Kokhirova, 2009). Furthermore, the meteoroids' sizes were selected randomly from a flat distribution in the logarithm of their radii, in the range $s = 100 \mu\text{m}$ to $s = 1$ mm, except for cases 8 and 9 (see Section 3.4.3), where we only simulated meteoroids with radii $s = 50 \mu\text{m}$. We emphasize that our knowledge of the actual particle distribution in the stream is highly biased towards hundred micron sizes, due to the daytime nature of the Arietids shower and detectability mostly by radar techniques. The size range chosen is not meant to reflect the expected size distribution, but rather allows us to efficiently explore the differential dynamical evolution of radar and visual meteoroids and to examine a possible mass segregation across the activity profile of the shower.

We assume that meteoroid ejection starts when the clones are within 3 AU from the Sun (i.e the heliocentric distance at which water ice begins to sublimate (Delsemme, 1982)). The meteoroid ejection, as a function of the heliocentric distance and ejection speed was modeled according to Brown and Jones (1998), where the ejection speed is given by:

$$V_{ej} = 10.2 r^{-1.038} \rho^{-1/3} R_c^{1/2} m^{-1/6} \text{ (m/s)} \quad (2)$$

where r is the heliocentric distance in (AU), ρ is the bulk density of the meteoroid in (g cm^{-3}), R_c is the radius of the comet nucleus in (km) and m is the mass of the meteoroid in (grams). The meteoroids are ejected with speeds, distributed isotropically on the

Table 2
The various cases used for meteoroid ejection throughout our forward simulations of 96P. Cases 1–3 correspond to meteoroid ejections before the chaotic region (based on the backward integrations), whereas cases 4 through 9 (see Fig. 3) are well within the chaotic zone. Cases 5 and 7 account for a variable dust production rate, of the clones of 96P/Machholz, as a function of time. In case 5, 3000 meteoroids per clone are ejected between 6500 BC and 3000 BC and 1000 meteoroids per clone between 3000 BC and the present. In case 7, 5000 meteoroids per clone are ejected between 10,000 BC and 6500 BC, 3000 meteoroids per clone between 6500 BC and 3000 BC and 1000 meteoroids per clone between 3000 BC and the present. Cases 8 and 9 correspond to meteoroid ejection from 10 different clones of 96P/Machholz, at a single perihelion passage.

Case №	Epoch of ejection	Ejection every N peri.	Number of active perihelion returns (N_p)	Number of meteoroids ejected over N_p (N_e)	Total number of ejected particles ($N_{tot} = N_p \times N_e$)
1	1000 CE	$N = 5$	38	2500	$\approx 9.5 \times 10^4$
2	0 CE	$N = 5$	76	2500	$\approx 1.9 \times 10^5$
3	3000 BCE	$N = 10$	95	5000	$\approx 4.7 \times 10^5$
4	6500 BC	$N = 10$	160	500×10 clones	$\approx 8 \times 10^5$
5	6500 BC	$N = 10$	160	Variable dust prod.	$\approx 2.9 \times 10^6$
6	10,000 BC	$N = 10$	226	500×10 clones	$\approx 1.1 \times 10^6$
7	10,000 BC	$N = 10$	226	Variable dust prod.	$\approx 6.2 \times 10^6$
8	20,000 BC	$N = 1$	1	$(5 \times 10^4) \times 10$ clones	5×10^5
9	30,000 BC	$N = 1$	1	$(5 \times 10^4) \times 10$ clones	5×10^5

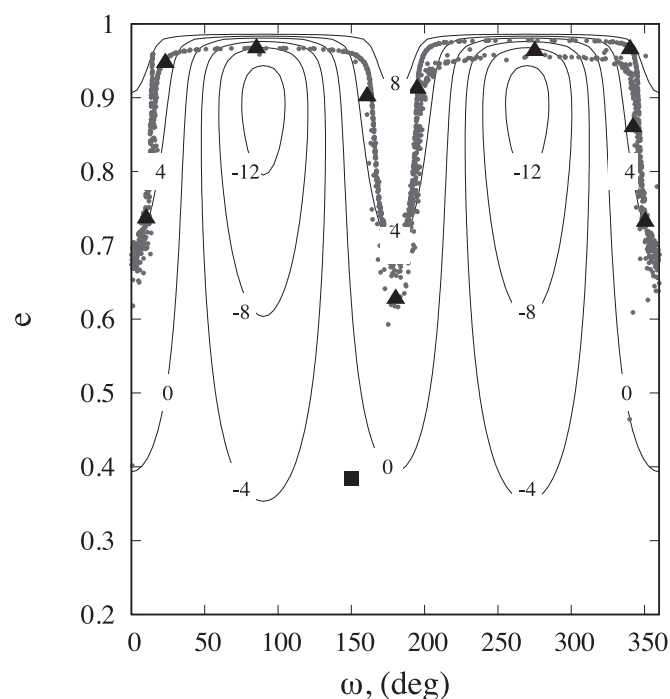


Fig. 4. Past Kozai type evolution of the orbit of 96P (black dots), for 20,000 years, across the lines of different values for the energy C in the Kozai resonance (solid lines). The black triangles indicate suitable clones, selected for forward integration and meteoroid ejections. The black square represents a sample "bad" clone, which we do not use for meteoroid ejection.

sunlit hemisphere, with dust production rate assumed to be uniform in time of the clones of the comet (a weighting by perihelion distance will be added later).

The equations of motion of the meteoroids along, with their parent clones, are integrated forward in time using Chambers' hybrid symplectic scheme (Chambers, 1999), until the present. The size of the meteoroids is considered in the dynamics via the standard β -parameter and the Poynting–Robertson drag, where $\beta = F_R/F_G$ is the ratio of the solar radiation pressure to the solar gravity. The magnitude of the β -parameter is given by Burns et al. (1979) as:

$$\beta = \frac{F_R}{F_G} \approx 5.7 \times 10^{-4} \frac{Q_{pr}}{\rho s}, \quad (3)$$

where ρ is the density of the meteoroid in kg/m^3 , s is the meteoroid radius in meters and Q_{pr} , which we assume to be unity

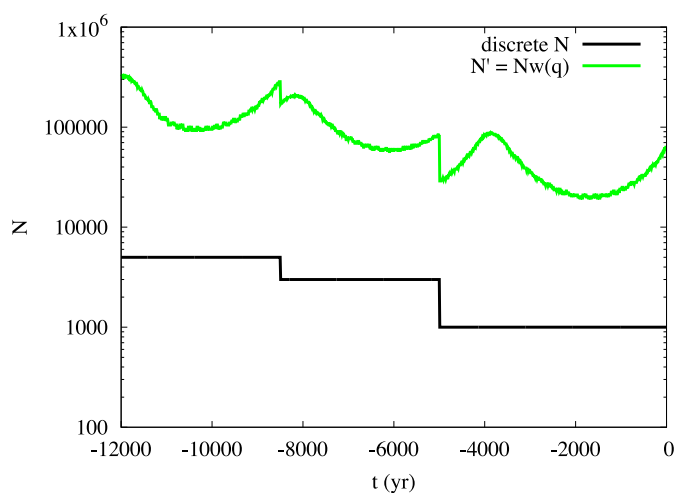


Fig. 5. Assumed variability of the meteoroid production rate for cases 5 and 7 in Table 2, starting in 10,000 BC and continuing until the present. The black line indicates discrete meteoroid ejections, with 5000 meteoroids per clone ejected between 10,000 BC and 6500 BC, 3000 meteoroids ejected between 6500 BC and 3000 BC and 1000 meteoroids between 3000 BC and the present. The green curve is a weighting of the discrete ejection as a function of the perihelion distance of the parent. The weighting scheme is adopted from Jones (2003). (For interpretation of the references to colour in this figure legend, the reader is referred to the web version of this article.)

(= 1), is non-dimensional coefficient representing the scattering efficiency of meteoroids. Furthermore, due to the extreme amplitude of the perihelion distances of both comets, P/1999 J6 and 96P/Machholz, we also accounted for general relativistic effects, even though both comets spend a very short time in the vicinity of the Sun, compared to their orbital periods.

3.4.2. Meteoroid ejection from parent candidate #1: P/1999 J6

To test child–parent relationship between the daytime Arietids and P/1999 J6, we considered five different origin epochs of the shower from P/1999 J6. Case 1 – with meteoroid production onset in 150 AD, case 2– for ejection in 350 AD, case 3 – for ejection in 500 AD, case 4 –for ejection in 700 AD and case 5 for meteoroid ejection in 950 AD, see Table 1. These meteoroid ejection epochs were chosen based on the work by Sekanina and Chodas (2005), who proposed that first precursors of comet P/1999 J6 and daytime Arietids may have separated from a common progenitor at these epochs. The ejected meteoroids as well as their ejection velocities were modeled as described in Section 3.4.1.

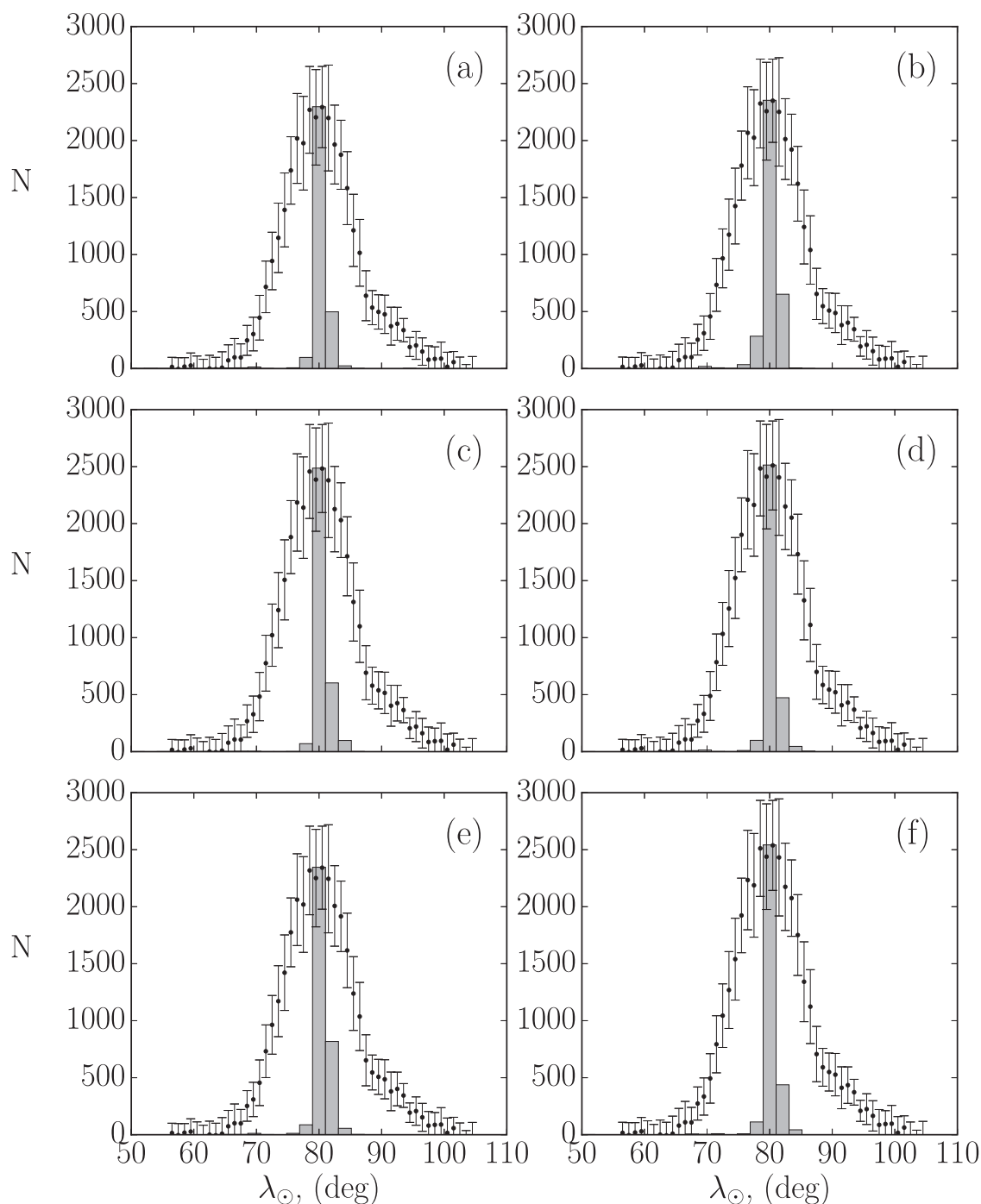


Fig. 6. Simulated activity profile for the daytime Arietids, at the present, for meteoroid ejection for case 1 (meteoroid ejection from P/1999 J6, between 100 AD and the present) and for six different clones panel (a), (b), (c), (d), (e) and (f), superimposed over the normalized observed profile by the CMOR (black dot with error bars). The observed profile is a stack for the years of 2002–2013 and includes meteoroids, equivalent to radar meteors of radar magnitude +6.5. The error bars in the observed profile correspond to 1σ from Bruzzone et al. (2015). For the theoretical profile, only meteoroids presently approaching the Earth's orbit within 0.01 AU have been considered.

Due to the stochastic nature of the orbital evolution of P/1999 J6 once we go more than 500 years into the past (see Fig. 2) we chose to eject meteoroids from 9 different clones of the comet as well as the nominal orbit of P/1999 J6. The selected clones have orbits located near the nominal trajectory in the phase space of the orbital elements. This selection was made on the basis that meteoroids with orbital elements completely different from nominal orbit are less likely to return close to the present orbit of P/1999 J6. Starting at each of the initial epochs in Table 1, a set of 250 meteoroids are released from each of the 10 clones of P/1999 J6 resulting in 2500 meteoroids at every fifth perihelion

return of the clones, or equivalently roughly every 30 years. For each case, the procedure is followed until the present with the number of meteoroids increasing by 2500 during each fifth perihelion return. We thus, effectively assume uniform cometary activity over the period of interest. This results in a synthetic meteoroid stream, at the present, consisting of a different number of particles $N_{tot} = N_p \times N_e$, as a function of the initial meteoroid ejection onset epoch (see Table 1).

Following the forward evolution of the orbits of the Arietid meteoroid stream, we imposed a perihelion distance limit, inside which the particles were considered “dead”, and thus removed

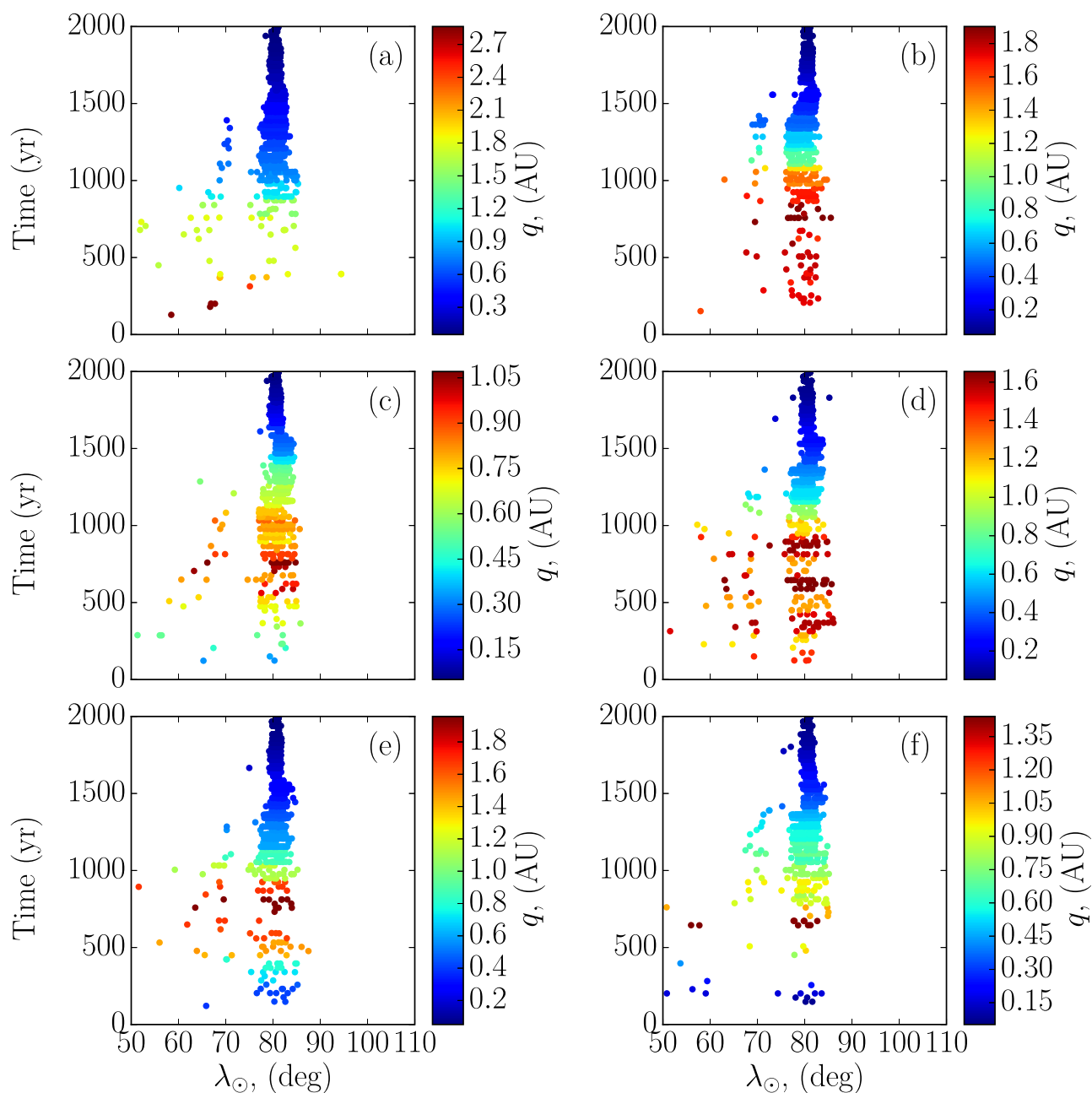


Fig. 7. The present distribution of the solar longitude λ_{\odot} of meteoroids, as a function of the ejection epoch in the common era, for case 1 (meteoroid ejection from P/1999 J6, between 100 AD and the present). The color bar corresponds to the perihelion distance (q) of the meteoroids at the time of ejection. Only meteoroids approaching the Earth's orbit within 0.01 AU have been considered. Six different clones of P/1999 J6 are shown, following the naming in Fig. 6.

from the stream. The cut-off distance was chosen to be $q = 0.025$ AU (or $\approx 5 R_{\odot}$), based on the physical ability for a meteoroid to survive at such low perihelion distances without being completely evaporated by solar heating (Peterson, 1971). We do not, however, have a priori knowledge on the exact chemical composition and physical strength of the daytime Arietid meteoroids, primarily because of the limited number of optical observations. However, assuming a genetic relationship between the Arietids and Quadrantids (e.g., McIntosh, 1990; Ohtsuka et al., 2003; Wiegert and Brown, 2005), it seems reasonable to assume a similar composition. We note, however, that due to the lower perihelion distance of the Arietids as compared to the Quadrantids, it is expected that the former to be relatively depleted of volatiles and more compact. Thus, a perihelion cut-off distance of $\approx 5 R_{\odot}$ seems reasonable, so we do not unintentionally remove potential Arietids from

the stream. Furthermore, we did not model particle sublimation effects near the Sun, nor did we account for the Lorentz force in the equations of motion of the meteoroids.

3.4.3. Meteoroid ejection from parent candidate # 2: 96P/Machholz

To test the parent-child relationship between the daytime Arietids and comet 96P/Machholz, we followed an approach similar to the case of P/1999 J6. However, due to the lengthy backward integrations (see Fig. 3) and the onset of chaos approximately 7500 years into the past, it is difficult to obtain meaningful results well in the chaotic region. Therefore, we constrain ourselves to epochs more recent or equal to 10,000 BC (a time scale that is shorter than the dynamical and physical lifetime of short period comets (cf. Section 3.3), and thus obtain a lower limit as to the age of the daytime Arietids. Furthermore, similar to the case with

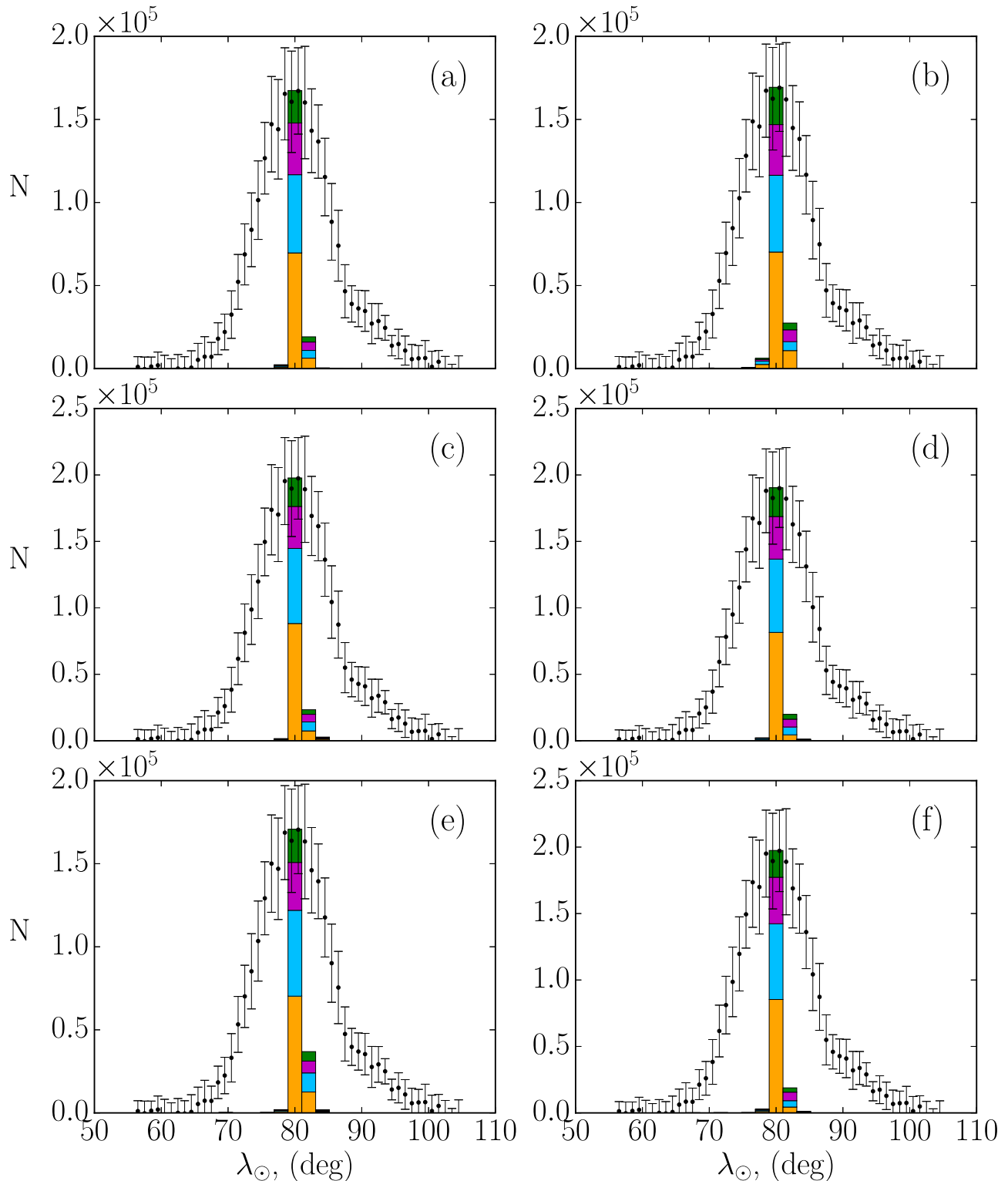


Fig. 8. The weighted activity profile for the daytime Arietids, at the present, as a function of the perihelion distance of the parent during meteoroid ejection for case 1 (meteoroid ejection from P/1999 J6, between 100 AD and the present). The profiles are presented for six different clones – panels (a), (b), (c), (d), (e) and (f), superimposed over the observed profile by the CMOR (black dot with error bars) for meteors brighter than radio magnitude of +6.5. The error bars in the observed profile correspond to 1σ . The four different colors in each stacked histogram denote particles of various size bin (expressed in terms of particles β -parameter). The “yellow” color correspond to $\beta = (2 \times 10^{-4} - 6.5 \times 10^{-4})$, “blue” $\beta = (6.5 \times 10^{-4} - 1.1 \times 10^{-3})$, “magenta” $\beta = (1.1 \times 10^{-3} - 1.55 \times 10^{-3})$, and “green” $\beta = (1.55 \times 10^{-3} - 2 \times 10^{-3})$. Effectively, the “yellow” color corresponds to the smallest and the “green” color to the largest particles, respectively. For the theoretical profile, only meteoroids presently approaching the Earth’s orbit within 0.01 AU have been considered. (For interpretation of the references to colour in this figure legend, the reader is referred to the web version of this article.)

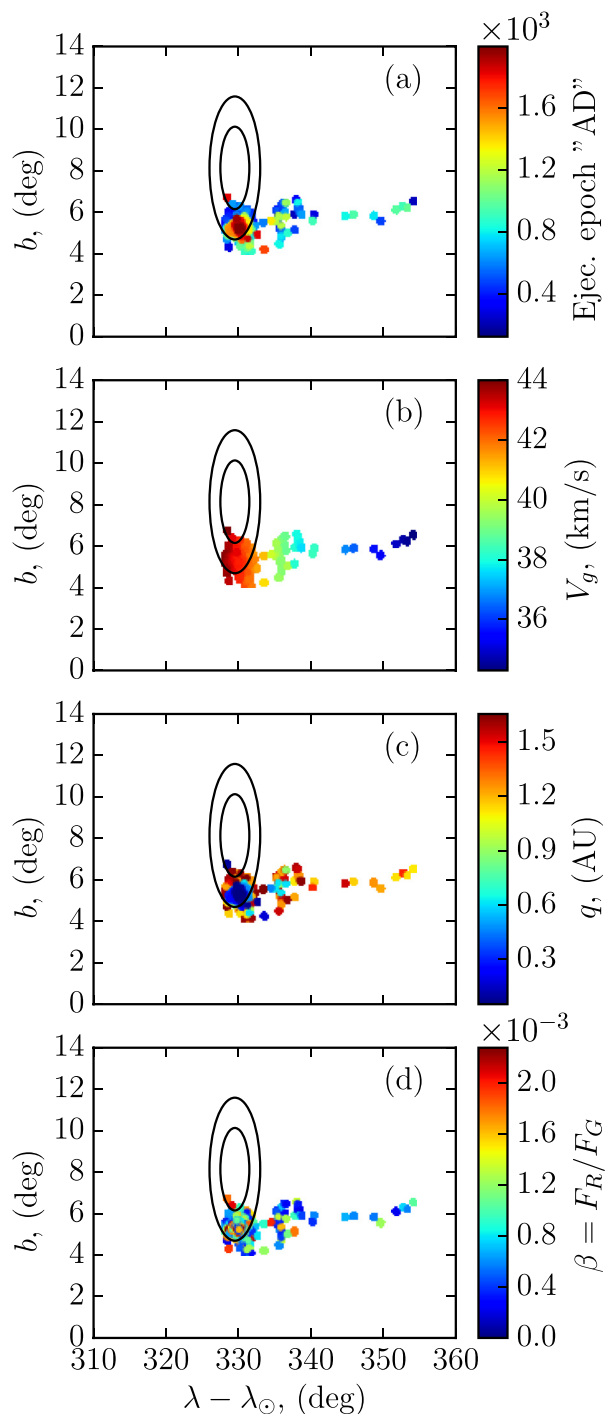


Fig. 9. Radiant position of the simulated daytime Arietids (color dots) for case 1 (meteoroid ejection from P/1999 J6, between 100 AD and the present) in Table 1 and for clone (b) in Fig. 8, superimposed over the observed radiant position by CMOR (black circles). The radiant position is given in sun-centered reference frame with coordinates - the sun-centered longitude $\lambda - \lambda_{\odot}$ and ecliptic latitude b . The two circles correspond to 68% and 95% confidence region respectively. The observed radiant includes meteors to a limiting magnitude +6.5 and is adapted from Bruzzone et al. (2015). The individual simulated radiants are color coded in terms of ejection epoch - panel (a), geocentric velocity V_g - panel (b), perihelion distance q at time of ejection - panel (c) and meteoroid β -value in panel (d). For the theoretical individual radiants, only meteoroids presently approaching the Earth's orbit within 0.01 AU have been considered.

P/1999 J6, meteoroids were modeled as described in Section 3.4.1. The parameters of the simulations were otherwise the same as earlier, except for a time step of integrations being $\delta t = 12$ hours.

Here, we considered 9 different meteoroid ejection onset epochs. These epochs are divided into two groups: (1) epochs before the orbit of 96P becomes chaotic, based on the backward integrations and (2) epochs in the chaotic region. The reason for this division is that we use two different approaches in selecting representative clones of 96P, which will be used for forward modeling of meteoroid ejection.

The first group of ejection epochs were chosen as 1000 CE, 0 CE and 3000 BCE respectively. We refer to these epochs as “case1”, “case2” and “case3” (see Table 2). In cases 1–3, the meteoroids were released from the nominal orbit of 96P/Machholz. The use of the nominal orbit seems plausible as in this time frame we do not see large dispersion in the orbital elements of the clones of the comet (Fig. 3). Moreover, the median values of the orbital elements of the clones are a good representation of the nominal orbit, at any given epoch from the present back until 5500 BCE. In cases 1–2, the meteoroids were released from the nominal orbit of 96P at every fifth perihelion return of the parent, whereas in case 3 at every tenth perihelion return. To maintain uniform cometary activity of 96P/Machholz over these time intervals, we double the number of meteoroids ejected per perihelion for case 3, in order to compensate for the greater interval between active perihelion returns.

In cases 4, 5, 6, 7, 8 and 9 the meteoroids are released from 10 different clones of comet 96P/Machholz, instead of the nominal orbit, due to the chaos beyond 5500 BC. The clones are selected based on their Kozai evolution, so that they lie on or close to the nominal Kozai trajectory of 96P in $(e - \omega)$ space (see Fig. 4). The Kozai energy C is given by e.g., Kinoshita and Nakai (1999) as:

$$C = (2 + 3e^2)(3 \cos^2 i - 1) + 15e^2 \sin^2 i \cos 2\omega, \quad (4)$$

where e is the eccentricity, i is the inclination and ω is argument of perihelion of the orbit respectively. Fig. 4 shows the theoretical Kozai cycle of comet 96P, in $(e - \omega)$ space, for different value of the Kozai energy integral C (Eq. (4)), with the actual trajectory of the comet and 10^3 clones superimposed over the calculated curves. It is to be noted that the evolution of 96P does not preserve the nominal Kozai energy precisely, as shown in Fig. 4. The reason for that may be due to close encounters with Jupiter or proximity of the orbit of 96P to a mean motion resonance with Jupiter, none of which are accounted for in the Kozai formalism. We have also indicated the sample of suitable clones that we use for meteoroid ejection and one “bad” clone that we discard in our simulations.

Similar to case 3, the meteoroids were released at every 10 perihelion returns, or roughly every 60 years, with 5000 particles equally distributed between the clones (see Table 2). In cases 4 and 6, we maintained a uniform meteoroid production rate, with (500 meteoroids/perihelion passage/clone \times 10 clones = 5000 meteoroids per perihelion passage). However, cases 5 and 7 are somewhat different, assuming a variable dust production rate for the clones of 96P/Machholz (see Fig. 5). For cases 5 and 7, we investigate a simple model of decreasing cometary activity: 5000 meteoroids ejections per clone for the time interval 10,000 BC – 6500 BC, 3000 meteoroids per clone between 6500 BC and 3000 BC and 1000 meteoroids per clone between 3000 BC and the present. The goal is to try to better match the much older “wings” of the activity profile of the Arietid shower. The motivation for this scenario does not seem unreasonable i.e. to expect that cometary activity to decrease over time, in particular over a time scale of a few thousand years, given the short orbital period of 96P. However, we emphasize that this scenario may break down if there was fragmentation in the past evolution of 96P, which is generally accompanied with enhanced dust production. The latter has been observed for several split comets, e.g. comet 73P/Schwassmann-Wachmann 3 which broke apart in 2006 and showed an increased

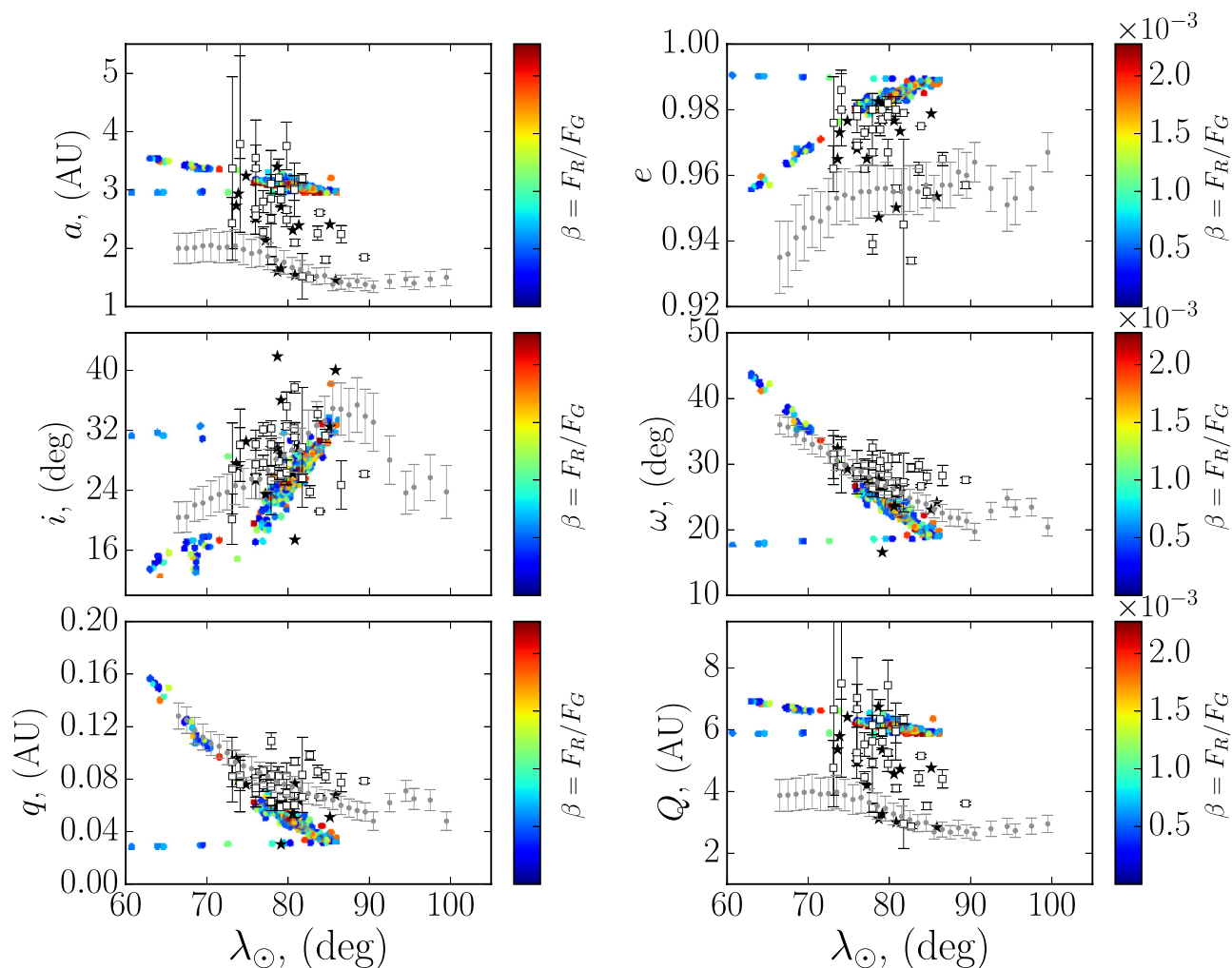


Fig. 10. Distribution of the mean orbital elements, semi-major axis a , eccentricity e , inclination i , argument of perihelion ω , aphelion distance Q and perihelion distance q of the Daytime Arietids as a function of the solar longitude. Individual color dots correspond to simulated meteoroids, ejected from clones of P/1999 J6 starting in 150 CE (case 1), where the color coding is in terms of the meteoroids' β -values. The open squares with $1-\sigma$ error bars correspond to 31 video Arietids, detected between 2011–2012 and are taken from the CAMS data (Jenniskens et al., 2016). The grey dots with $1-\sigma$ error bars are derived from a decadal survey of the Arietids by CMOR (Bruzzone et al., 2015) and the black stars correspond to 14 individual TV events by (SonotaCo, 2009).

brightness in the light curve, likely attributed to increased gas and dust emission (e.g., Sekanina, 2005).

At the end of the simulations, these discrete meteoroid ejection epochs are weighted by the perihelion distance of the parent at the time of meteoroids' ejection. The reason for that weighting is to account for the higher dust production rate at stages of very low perihelion distances, due to the greater proximity to the Sun. The weighting parameter that we use was adopted from Jones (2003) and is given by:

$$w = \frac{\theta_c(1-e)^2}{q^2\sqrt{1-e^2}}, \quad (5)$$

where θ_c is the true anomaly of the comet within which it becomes active, e is the eccentricity of the orbit and q is the perihelion distance of the comet in AU, at the time of meteoroid ejection.

We emphasize that the variability of the activity of 96P/Machholz is not an unreasonable assumption, as it is unlikely that the comet has maintained a constant activity since 10,000 BC. There are various mechanisms, that lead to decrease in cometary activity over time, such as volatile depletion and formation of an inert crust on the surface of comets (e.g., Rickman et al., 1990). However, we do not know the exact function or rate

at which the activity of 96P/Machholz has decreased over time, instead our approach provides grounds to test the hypothesis of decreasing activity over time.

Case 5 is similar to case 7, with the major difference being the initial meteoroid ejection onset time 6500 BC. Furthermore, in order to be consistent with case 7, we ejected 3000 particles per clone between 6500 BC and 3000 BC and 1000 particles per clone between 3000 BC and the present. In general, there are myriad of parameters that can be adjusted to reflect various meteoroid ejection scenarios, however the exact combination of these variables are not known. We thus, only investigate a few simple hypotheses.

Finally, cases 8 and 9 were designed to test whether the discrepancy between the orbital elements of the daytime Arietids, as derived from radar and optical surveys, can be attributed to the Poynting–Robertson drag (e.g., Robertson, 1937; Burns et al., 1979), given a sufficiently long period of time. The explicit change in the semi-major axis and eccentricity of the orbit due to the Poynting–Robertson drag can be found in (e.g., Klačka, 2004) which we omit here. Bruzzone et al. (2015) found that the values of semi-major axes and eccentricities for radar and optical size particles converged to similar values between 10^4 and 10^5 years, i.e. the discrepancy between radar and optical size particles can be removed if Poynting–Robertson drag has acted over time scales greater than

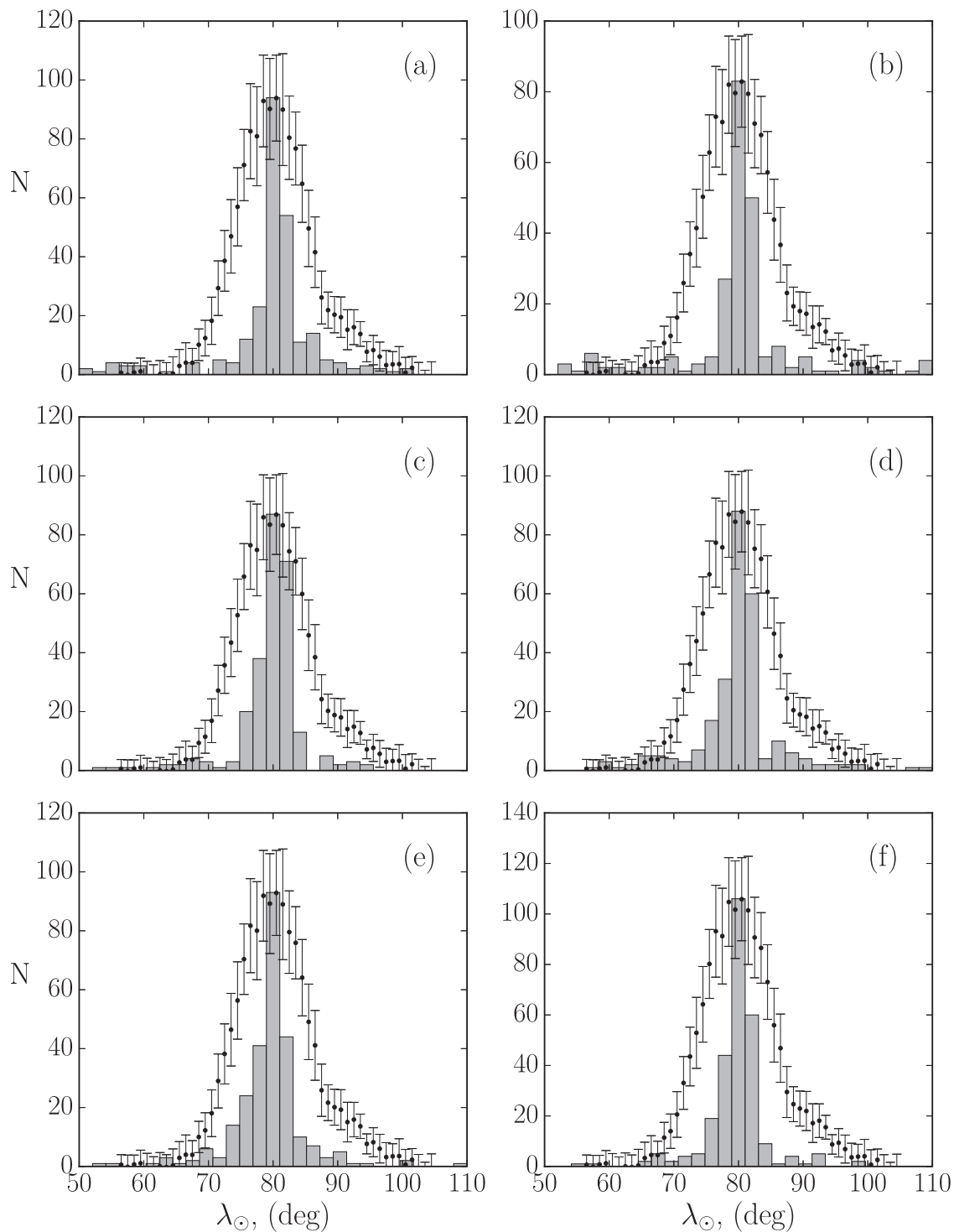


Fig. 11. The simulated unweighted activity profile for the present daytime Arietids for meteoroid ejection in case 6 from comet 96P. See Fig. 6 for details.

10,000 years. In their work Bruzzone et al. (2015) do not consider the gravitational influence of the Sun and planets on the meteoroids, and merely consider that the particles are subjected to only radiation effects from the Sun.

In the cases 8 and 9, we considered only meteoroids with radii $s = 50 \mu\text{m}$, with equivalent $\beta \approx 5 \times 10^{-3}$ being strongly affected by the solar radiation pressure. The density of the meteoroids and the ejection speeds were modeled as described in Section 3.4.1. In contrast to previous cases, 5×10^4 meteoroids were ejected at

a single perihelion passage and epoch centered at 20,000 BC and 30,000 BC (see Table 2) from 10 different clones of 96P/Machholz. We note that, the aim of cases 8 and 9, is merely to test whether the discrepancy of the semi-major axis and eccentricity can be attributed to the Poynting–Robertson drag alone. That is, given a sufficiently large time scale our goal is to investigate whether Poynting–Robertson drag can decrease the semi-major axis and eccentricity of $50 \mu\text{m}$ size Arietids (an extreme lower limit for CMOR sizes) to their presently observed values.

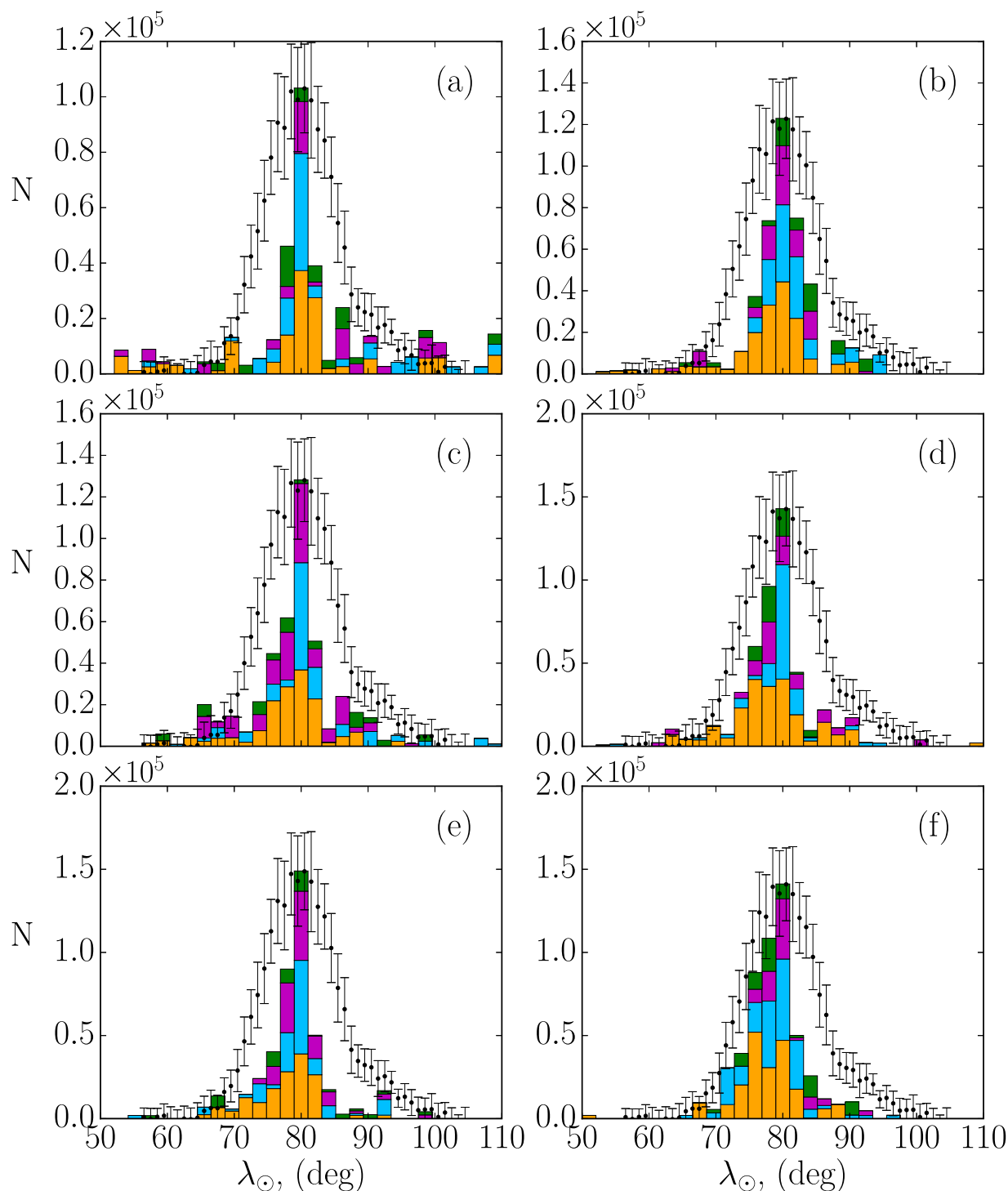


Fig. 12. The weighted activity profile for the daytime Arietids, at the present for meteoroid ejection from 96P, for case 6 in Table 2. Details as in Fig. 8.

The equations of motion were integrated forward in time, starting from each individual epoch 30,000 BC and 20,000 BC, until the present using the Chambers' symplectic scheme (Chambers, 1999). During the integrations we accounted for the gravitational influence of all eight planets, general relativistic effects due to the meteoroids' low perihelion distances as well as solar radiation pressure and Poynting-Robertson drag. However, we neglected the Lorentz force as well as the solar wind drag, as the latter forces are small (e.g., Leinert and Grün, 1990) compared to solar radiation pressure and Poynting-Robertson drag, for the particles of interest in this work.

4. Results

4.1. Parent candidate #1: P/1999 J6

In order to compare the observed and simulated characteristics of the daytime Arietids, we consider the simulated Arietids to be any meteoroids which have their orbital nodes within 0.01 AU from the Earth's orbit. This number was chosen somewhat arbitrarily as a compromise to avoid low meteoroid number statistics, though in reality only meteoroids actually hitting the Earth can be detected. Different works, related to the association of

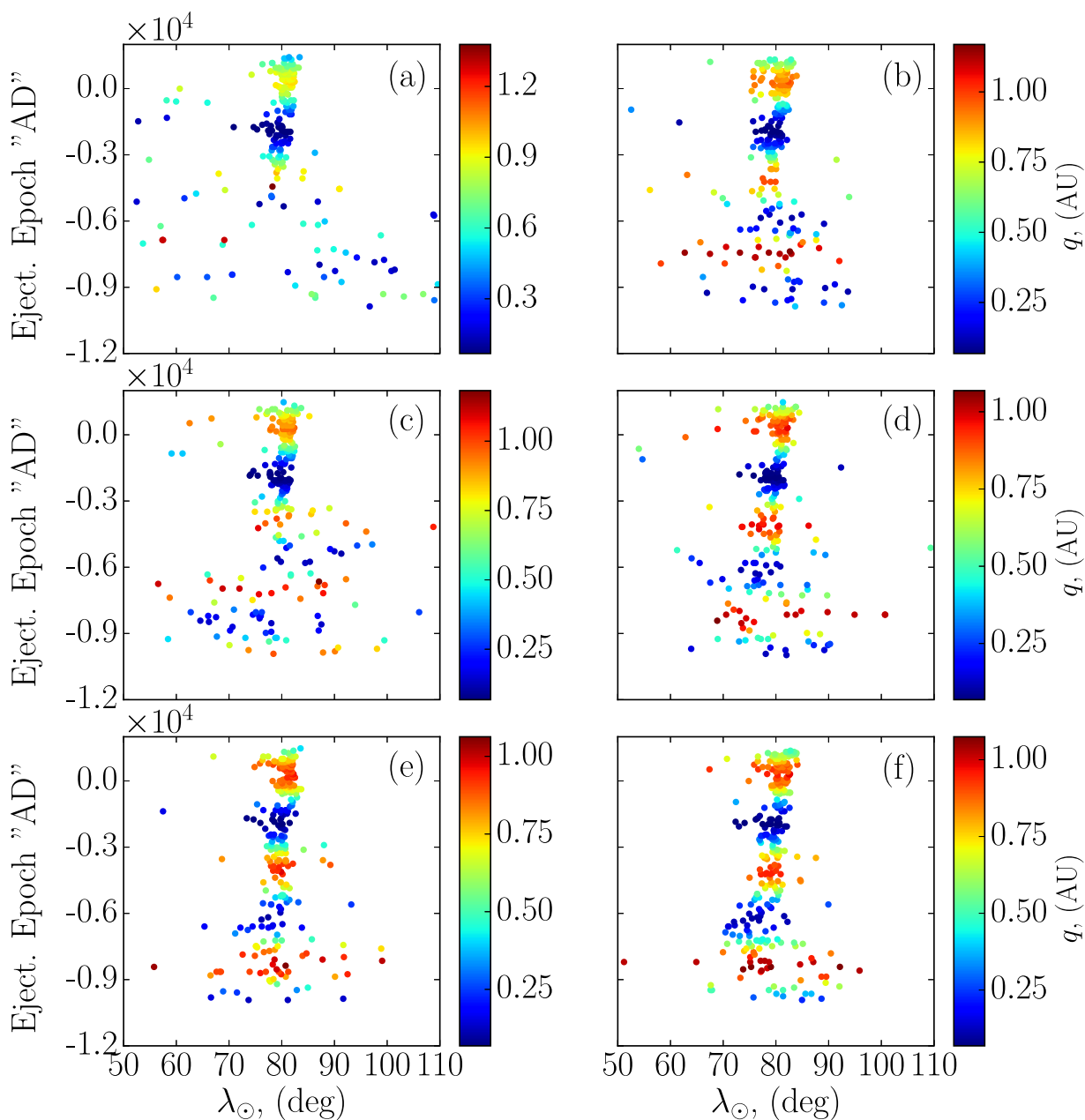


Fig. 13. The present simulated distribution of the solar longitude λ_{\odot} of meteoroids, for six clones of 96P, as a function of the ejection epoch, for case 6 in Table 2. Details as in Fig. 7.

meteoroid streams with a given parent, adopted different values generally ranging between 0.005 AU and 0.05 AU (e.g., Brown and Jones, 1998; Jenniskens and Vaubaillon, 2010; Neslušan et al., 2013).

Furthermore, we only present results for six clones out of ten and compare the simulated and observed characteristics of the daytime Arietids only for case 1 in Table 1. The rest of the cases yielded similar results which we decided to omit here. Fig. 6 presents the activity profiles for six different clones for meteoroid ejection in case 1. The combined profile is a stack of meteoroids of all sizes with radii between $s = 100 \mu\text{m}$ and $s = 1 \text{ mm}$, and we refer to that profile as the “unweighted” profile. In addition, superimposed is the observed activity profile of the Arietids by CMOR as an average from the years 2002–2013 (Bruzzone et al., 2015), including meteors to a limiting radio magnitude of +6.5. It is evident that the selection of different clones of P/1999 J6 has little

effect on the final results. The resulting profiles are too narrow to be consistent with the observations by CMOR. However, these profiles do not realistically capture the meteoroid population in the stream, as they assume a dust production rate independent of the perihelion distance of the parent at the time of meteoroid ejection. However, it is not unreasonable to expect that an increased supply of dust would be produced at lower perihelion distances. In order to examine this, we first examine a plot of the solar longitude λ_{\odot} of particles presently intersecting the Earth, as function of their time of ejection and their perihelion distance at the time of ejection (Fig. 7). Since 1200 CE, P/1999 J6 has had its perihelion distance below 1 AU, with extreme values of $\approx 0.1 \text{ AU}$. Thus, it is reasonable to expect that the dust released during these stages of very low perihelion distance should contribute relatively more to the stream than particles ejected at larger q . Therefore, we apply a perihelion-based weighting to the activity profile in order to

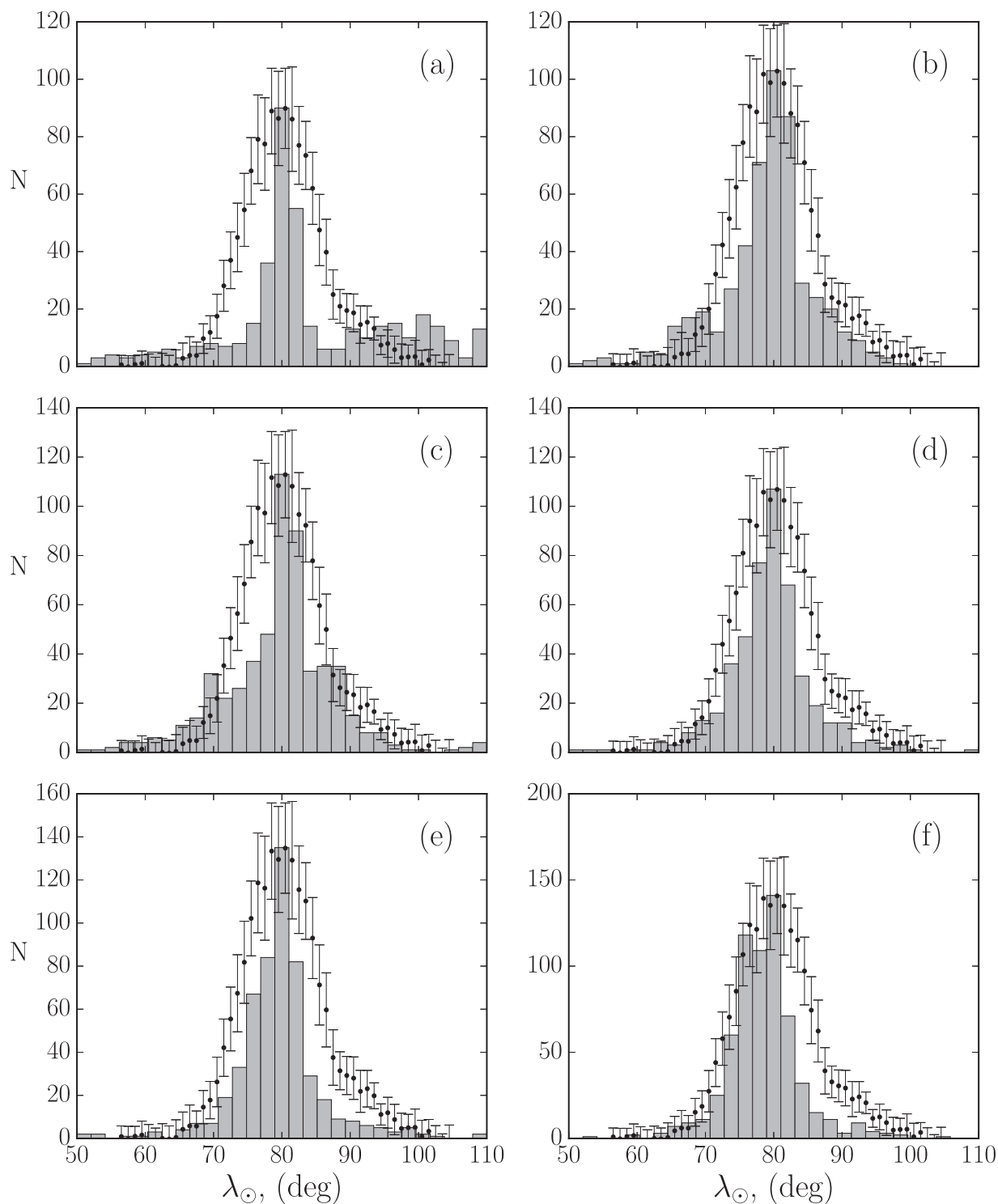


Fig. 14. Simulated unweighted activity profile for the daytime Arietids, at the present, for meteoroid ejection from 96P, for case 7. Details as in Fig. 6.

more realistically model the number of particles in the present activity profile. We hereafter refer to that profile as to the “weighted” profile. The weighting parameter that we use is given by Eq. (5)

Thus, the number of particles N'_i in the i th bin of solar longitude $\lambda_{\odot i} + \Delta\lambda_{\odot}$, as a function of their perihelion distance at the time of ejection, is:

$$N'_i = \sum_{j=1}^n N_{ij} w_j(q_j), \quad (6)$$

where N_{ij} is the j th particle in the i th bin with perihelion distance q_j at the ejection epoch, w_j is the weighting factor for a given perihelion distance q_j . The result of weighting of the activity profile is presented in Fig. 8. In order to check whether there is a particular mass sorting along the profile, the weighted activity profile also provides information of particle size in each bin. However, our results did not show any particular mass segregation as a function of solar longitude.

Regardless of the initial meteoroid ejection onset epoch, the activity profile resulting from P/1999 J6 results in a sharp

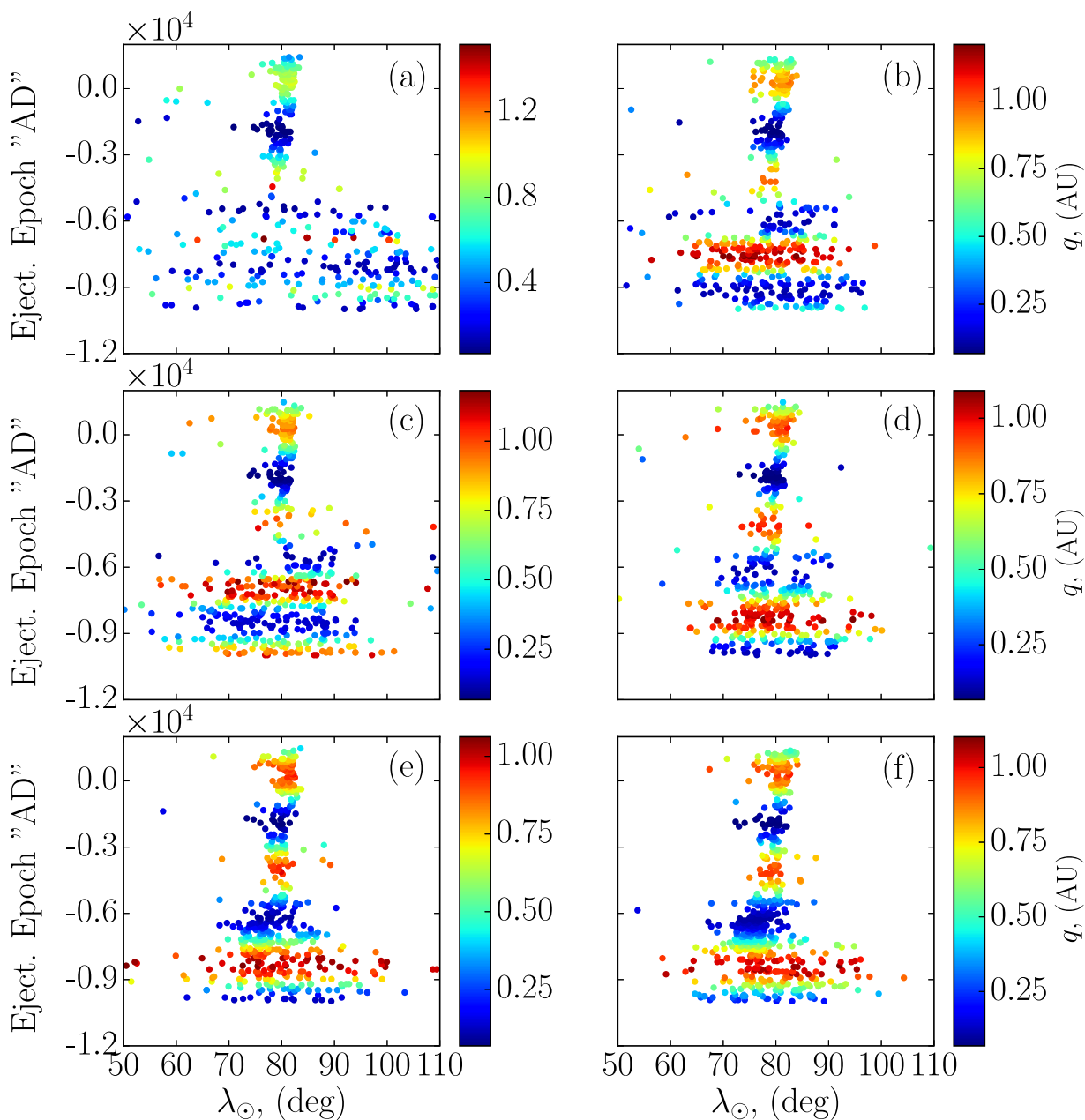


Fig. 15. The present distribution of the solar longitude λ_{\odot} of meteoroids, as a function of the ejection epoch for comet 96P, for case 7 in Table 2. Details as in Fig. 7.

maximum and very weak broader activity, which is inconsistent with the overall activity profile. The reason can be gleaned from Fig. 7 where it can be seen that only particles ejected prior to 1000 AD contribute to the wings of the activity profile. However, these meteoroids were ejected at larger perihelion distances and thus according to our weighting scheme they contribute less than the particles released in the last 1000 years. The result for the rest of our cases and clones yielded similar results. Due to the greater concentration of meteoroids near the peak of the activity profile $\lambda_{\odot} = 80.5^{\circ}$ (see Fig. 7), at any ejection epoch, the weighted activity profile will always result in a narrow sharp maximum, regardless of the perihelion distance weighting factor. In fact, the rest of the cases (cases 2–5) resulted in even narrower profiles due to the lack of particles to fill the wings. Thus, based on our simulations, comet P/1999 J6 alone can not explain the entire activity profile of the shower, though it may contribute to the core of the stream.

The simulated radiant position of the daytime-Arietids, from comet P/1999 J6, is presented in Fig. 9. The simulated radiant pro-

duced a relatively good match with the observations, except for a few particles outside the 95% confidence region. There is a lack of any mass segregation along the width of the stream as is evident from Fig. 9, which is also reflected in Fig. 8.

Fig. 10 shows the theoretical distribution of the orbital elements of the daytime Arietids assuming an origin from P/1999 J6 in 150 AD (case 1) for only one clone. It is evident that, there is a poor match in the present a , e and Q , with radar observations by CMOR and other radar measurements as given in Bruzzone et al. (2015). In fact, the simulated orbital elements are more consistent with TV and video observations which predict systematically higher values for a and e and Q , as compared to radar surveys. Poynting–Robertson drag in our simulation did not change the semi-major axis of the meteoroids enough to bring them close to the values observed by CMOR, over the time scale of our simulations. In summary, the conjecture that the daytime Arietids are solely associated with Marsden group of sunskirting comets was not supported by our simulations, though our results

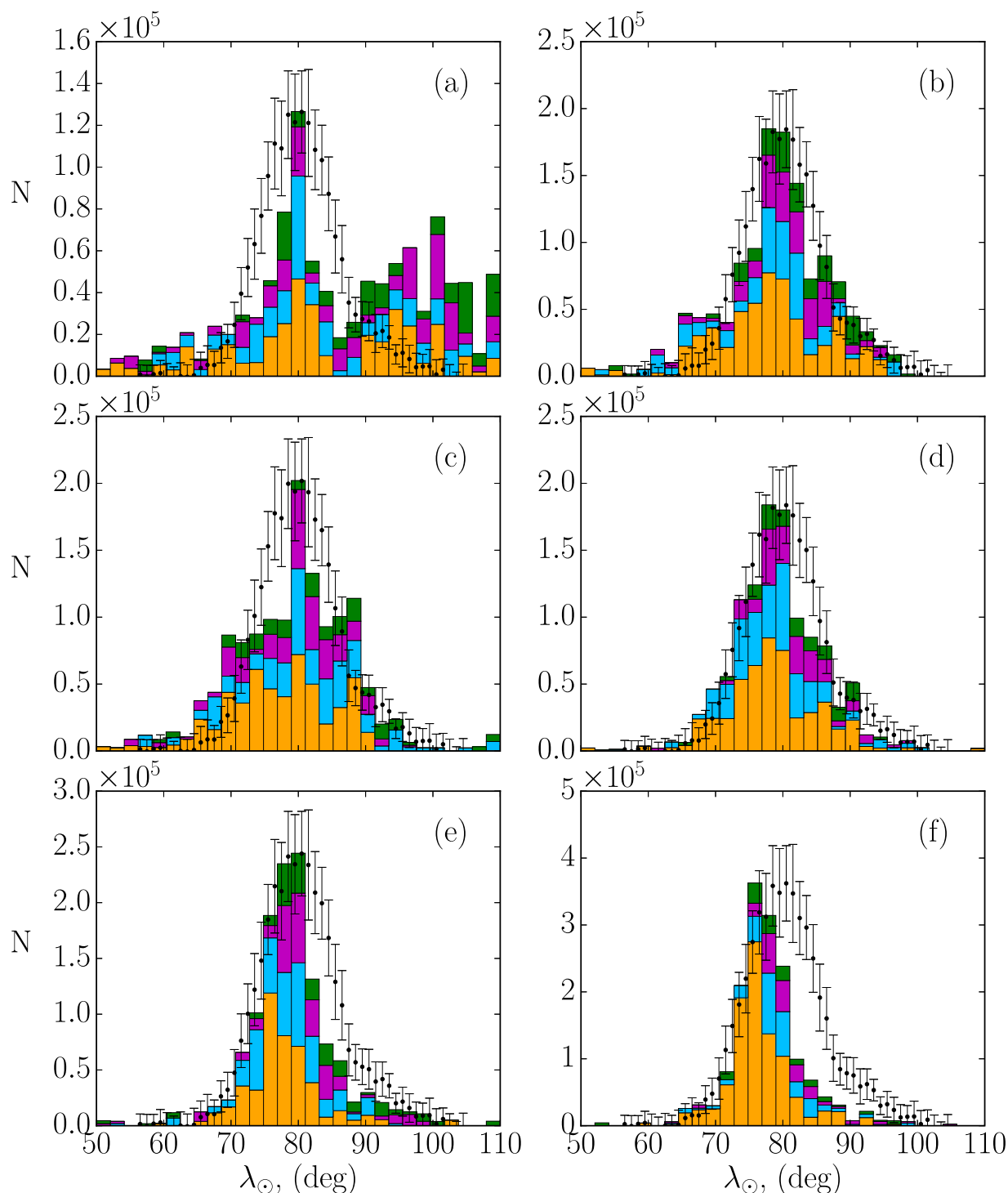


Fig. 16. The weighted activity profile for the daytime Arietids, at the present for meteoroid ejection from comet 96P, for case 7. Details as in Fig. 8.

indicate that comet P/1999 J6 could contribute to the peak of the shower.

4.2. 96P/Machholz

In this section we examine the hypothesis that comet 96P/Machholz is the parent of the daytime Arietids and present the results from the forward numerical simulations of meteoroids released from the comet. Similar to the previous section, we show results for only six clones. We present a detailed discussion of the

outcome of our simulations only for cases 5, 6 and 7 in Table 2 and provide a short discussion for the remaining cases which were similar in most respects.

4.2.1. Cases 6 and 7

In case 6 we assumed a uniform cometary activity for 96P/Machholz. Fig. 11 shows the individual theoretical “unweighted” activity profiles of the daytime Arietids, for meteoroid ejection onset in 10,000 BC (case 6 in Table 2), for six individual clones of 96P. Superimposed is the observed normalized profile by CMOR,

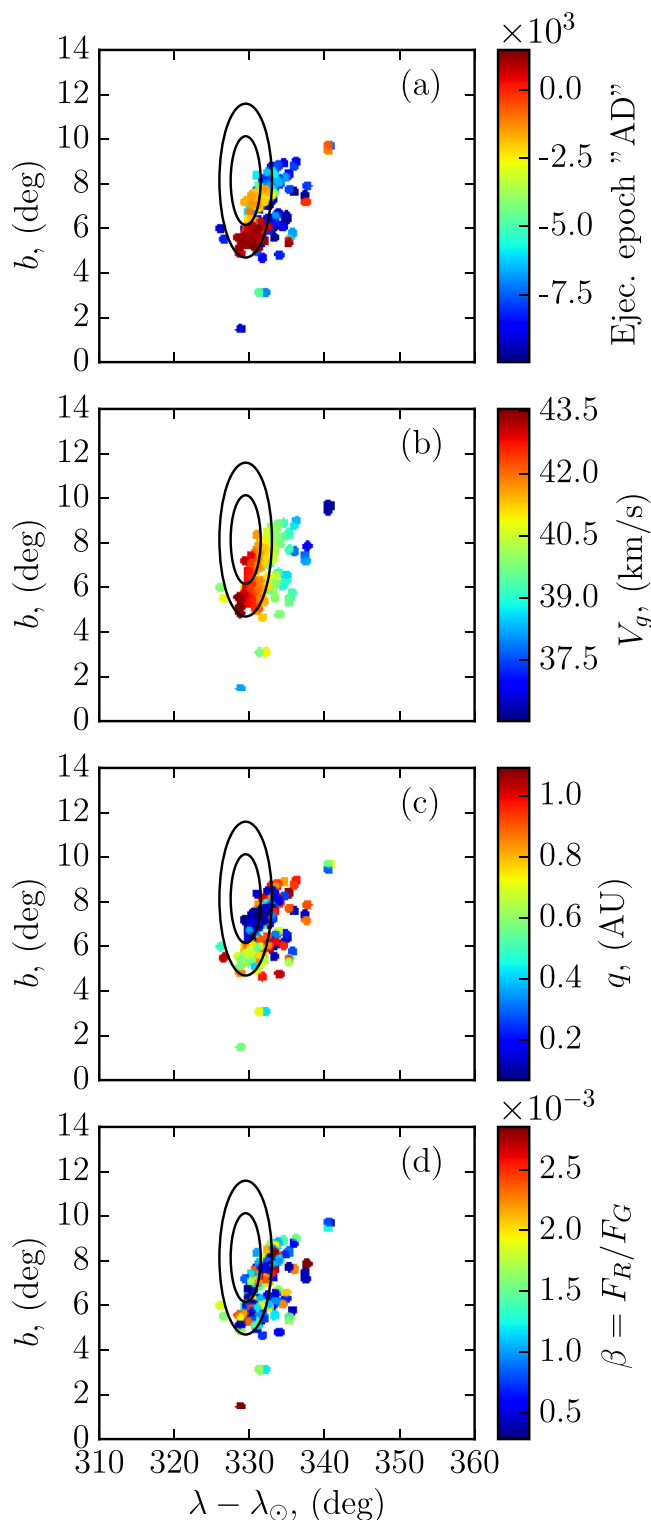


Fig. 17. Radiant position of the simulated daytime Arietids (color dots) for case 7 in Table 2 for clone (b) of comet 96P. Details as in Fig. 9.

as a stack for the years of 2002–2013. The unweighted profiles combine simulated particles of all sizes, with radii between $s = 100 \mu\text{m}$ and $s = 1 \text{ mm}$ which span mass ranges for both radar and TV/Video meteors.

It is evident that the peak of the activity profile is reproduced fairly well, while the resulting width of the profile is too narrow to be consistent with the observations. Similar to P/1999 J6 we applied a weighting scheme based on the meteoroids' perihelion dis-

tance at the time of ejection. The resulting “weighted” profiles, for the six clones of 96P/Machholz, are presented in Fig. 12.

The weighted profile produces a good match, though the wings are still not reproduced well. For example, clone (a), produced the worst match in our sample, with sharp peak and a lower background activity exceeding the observed width of the shower's profile. Clone (b), on the other hand, yielded the best fit although not entirely filling the wings. The reason for the discrepancy is the low number of particles away from the peak of the profile ($\approx 80.5^\circ$). Fig. 13 illustrates the situation by showing the time of ejection and the perihelion distance of the parent at that time. The epochs of minimum perihelion distance are separated by ≈ 4000 years (half the period of the Kozai cycle, see Section 3.3), so these particles ejected at these times are expected to contribute more to the activity profile of the Arietids. However, the particle distribution at epochs of low perihelion distance tend to be tightly concentrated contributing to a narrow peak. There are some older particles dispersed enough to fill the wings, but this would require the comet to have had higher dust production at early times, a scenario which we will investigate next.

Assuming that 96P/Machholz has been captured into a short period orbit circa 10,000 BC, it is not unreasonable to expect that its activity level (dust and gas production rate) has changed over time, being more active in the past. In order to investigate that scenario, we modified case 6 (see Table 2 in Section 3.4.3), to reflect a decrease in the activity of 96P, according to Fig. 5. We refer to this scenario as case 7. Fig. 14 shows the unweighted activity profile of the daytime Arietids for case 7, and for six different clones. Relative to case 6, it produced a better fit to the observed profile by CMOR, matching the wings well. Similar to the previous case, however, this profile does not provide information about the particle size in each bin, nor does it capture the variability of the activity of 96P/Machholz. We therefore, apply the same weighting scheme, as in for case 6, to account for a higher dust production rate, expected during stages of lower perihelion distance. Fig. 15 shows the meteoroid distribution, presently approaching the Earth's orbit within 0.01 AU, as a function of their ejection epoch and perihelion distance at the time of ejection from six clones. The result of weighting the activity profile, as before, is presented in Fig. 16. It is evident that for some clones (b) and (e) the wings of the profile are reproduced fairly well, while for clone (a) the match was poor. The omitted clones also yielded relatively good matches typically consistent with the observed profile within the error bars.

The resulting simulated radiant position of the daytime Arietids for case 7 and clone (b) is shown in Fig. 17, superimposed over the observed mean radiant by CMOR. The fit to the observations is very good, with only a few particles being outside the 95% confidence region. It can be seen that the particles that are well outside the 95% confidence region hit the Earth with speeds below 38 km/s (panel (b) in Fig. 17), so that these meteoroids might not have been identified as Arietids by CMOR, or simply might not exist. Furthermore, we do not observe any mass segregation along the radiant (panel (d)), although there seems to be a slight correlation between the meteoroid ecliptic latitude b and the ejection epoch, where the latter differs by about 3° for youngest and oldest particles.

As was the case with the Marsden group comet P/1999 J6, simulations of 96P were not able to reproduce the distribution of all orbital elements of the daytime Arietids, as a function of the solar longitude λ_\odot as observed by CMOR. Fig. 18 shows the orbital elements according to our simulations superimposed over the observations by CMOR (Bruzzone et al., 2015), and 14 TV and 31 video daytime Arietids. Our simulations yielded systematically higher values for the semi-major axis a of the meteoroid compared to CMOR measurements. A similar outcome was observed for the eccentricity e and the aphelion distance Q , while the

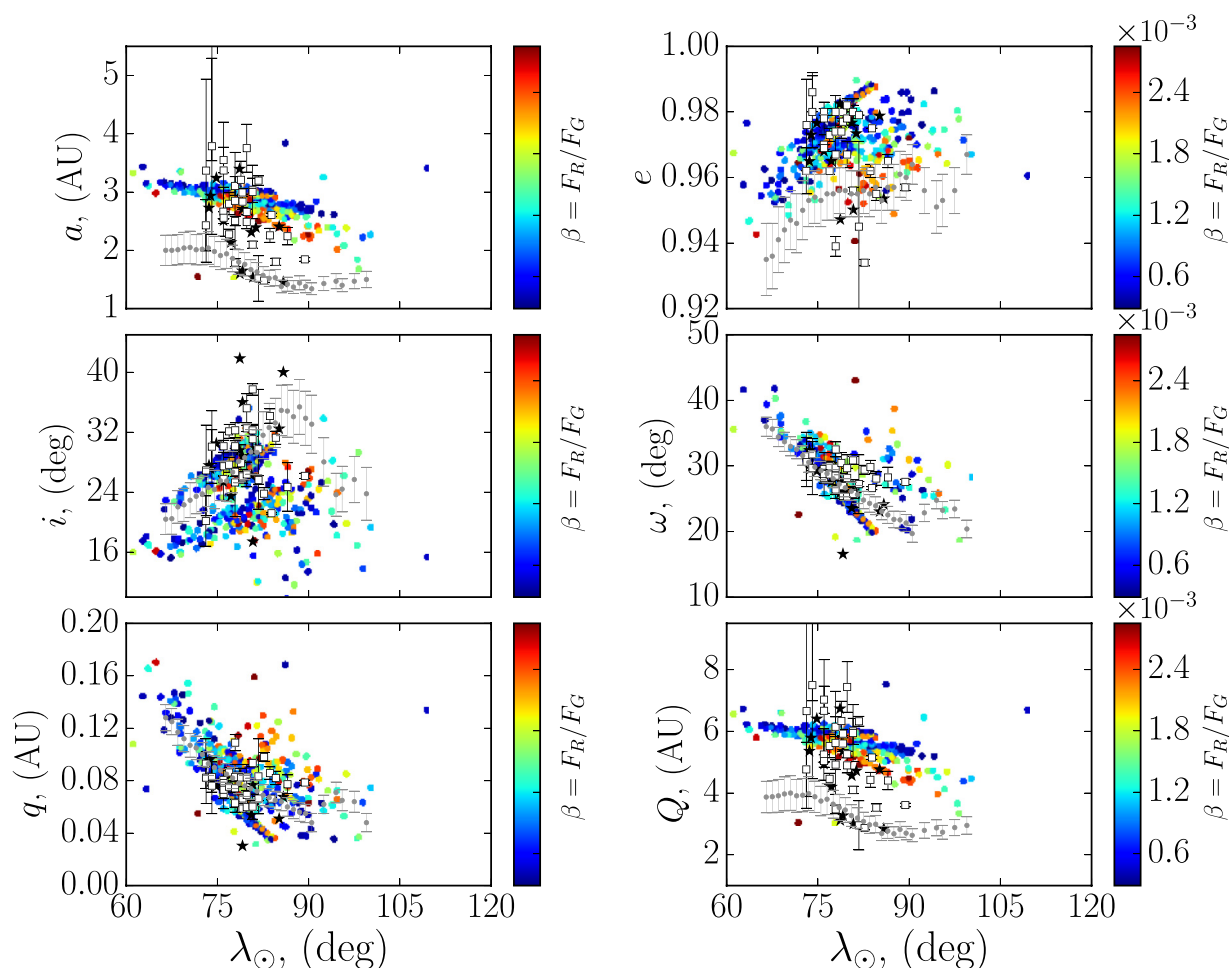


Fig. 18. Distribution of the mean orbital elements, of the Daytime Arietids as a function of the solar longitude, for meteoroid ejection from 96P (case 7). Details as in Fig. 10.

inclination i , argument of perihelion ω and the perihelion distance yielded a good fit to the radar data. Our simulations are more consistent with the optical surveys. Finally, all other clones which have been omitted here for convenience, resulted in very similar outcome, none being able to reproduce the observed distribution of the semi-major axis, eccentricity and the aphelion distance, with radar but resulting in a very good match with the optical surveys.

4.2.2. Case 5

In case 5, we used a similar approach to case 7, assuming a variable dust production for 96P, with 3000 meteoroids per clone, ejected between 6500 BC and 3000 BC and 1000 meteoroids per clone between 3000 BC and the present, see Table 2. Case 4, in our simulations, assumed a constant dust production rate over time and produced a narrow profile, inconsistent with the observed profile of the shower. The aim of case 5 is to check how well a variable dust production of 96P (similar to case 7) can reproduce the observed characteristics of the shower and to compare that to case 4. Fig. 19 shows the “unweighted” activity profile for six different clones in case 5, for particles with radii between 100 μm and 1 mm. It can be seen that the match is not as nearly good as in case 7, with all clones producing a relatively narrow peak and weak background activity. The reason for that can be inferred from Fig. 20, as the older particles are rather dispersed in nodal longitude, compared to particles ejected prior to 5000 BC. As a result, younger particles cause the peak to increase, whereas the dispersed older particles contribute only moderately to the wings.

As before, we apply the same activity weighting as used in the cases 6 and 7, to account for the rate of dust production as a function of the perihelion distance. The result of this weighting is presented in Fig. 21. Regardless of the weighting, the match between the observations and our simulations was poorer compared to case 7, with the wings of the theoretical profiles being too narrow to match the observations by CMOR. Case 4, in our simulations produced a similar outcome, though with somewhat narrower wings, compared to case 5. In addition, we do not observe mass segregation along the activity profile that could potentially explain the discrepancy in the distribution of the orbital elements as a function of the solar longitude, between the radar and optical surveys.

Fig. 22 shows the simulated individual radiant positions of the daytime Arietids for case 5 and for clone (b). The radiant position produced a good match with observations, as in case 7 (Fig. 17), though the width of the activity profile (Fig. 21) yielded a poorer fit to the observations. The lack of mass sorting along the radiant is also evident from the figure (panel (d)), although obviously there is a strong correlation between the radiant position and the particles geocentric speed (panel (b)), and somewhat lower correlation as a function of the ejection epoch (panel (a)) and perihelion distance at the time of ejection (in panel (c)). As in case 7, it is not unreasonable to expect that small particles with speeds below 38 km/s are not associated with the stream in the CMOR study, so the particles outside the 95% confidence region may have been too sparse and slow to be registered by CMOR, as a part of the shower.

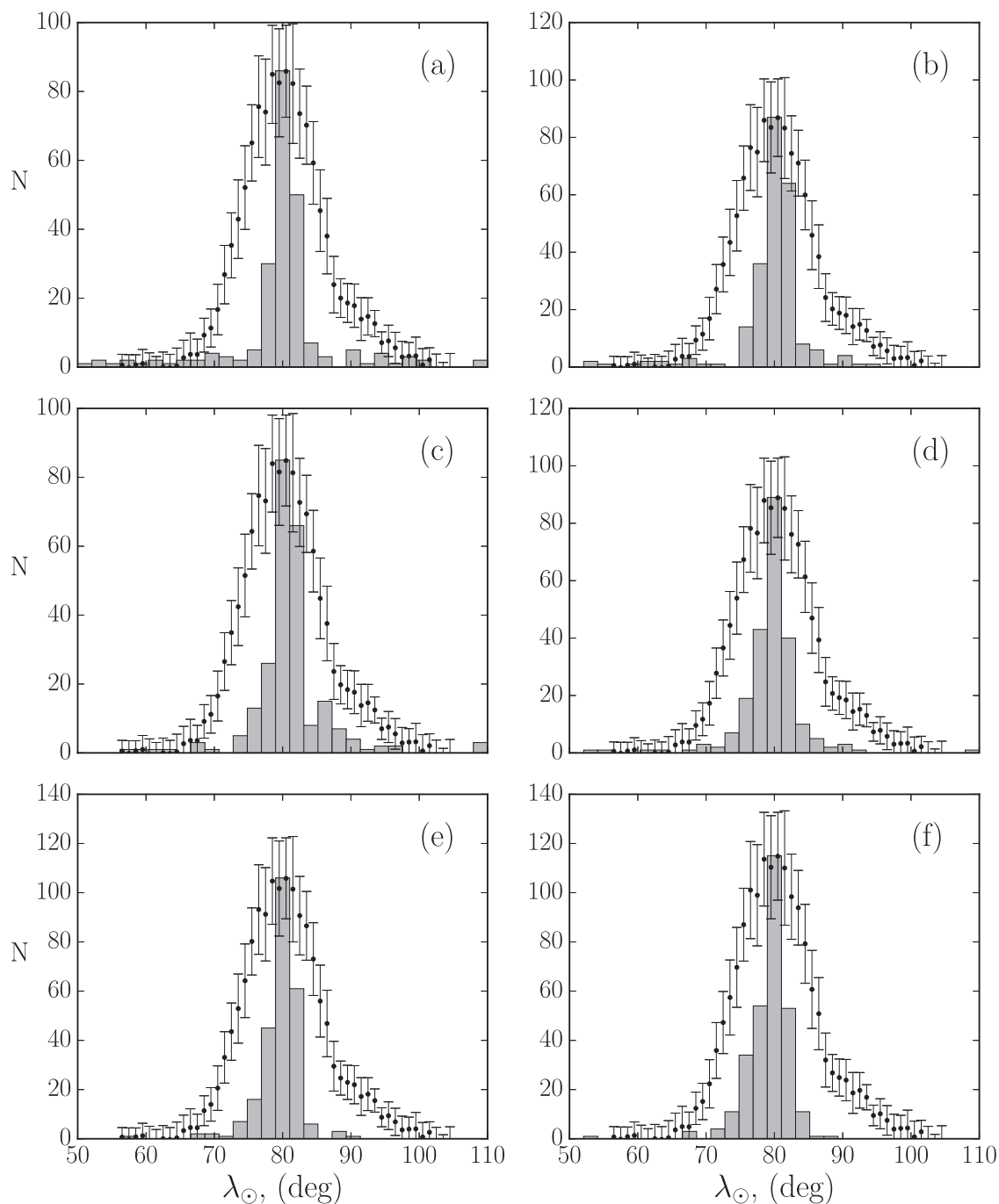


Fig. 19. Simulated unweighted activity profile for the daytime Arietids, at the present, for meteoroid ejection from 96P, for case 5 for six different clones. Details as in Fig. 6.

The distribution of the orbital elements, of meteoroids currently approaching the Earth's orbit within 0.01 AU, as a function of the solar longitude is presented in Fig. 23. These did not differ significantly from the previous cases. Some of the orbital elements, such as semi-major axis (a), eccentricity (e) and the aphelion distance (Q), of the simulated meteoroids, yielded systematically higher values, compared to CMOR survey. The effect of the Poynting–Robertson drag is too small to explain the orbit inconsistency between the radar and optical surveys, over these formation time periods. In fact, our simulated meteoroids matched better the 14 TV (SonotaCo, 2009) and the 31 CAMS (Jenniskens et al., 2016) events, although we observed a large dispersion among individual optically detected Arietids.

Assuming that the underlying mechanism of the formation of the daytime Arietids is due to a normal cometary outgassing, our results indicate that the origin of the stream is more consistent with comet 96P/Machholz, rather than the Marsden group of sunskirting comets (P/1999 J6). Moreover, our simulations indicate that age of the daytime Arietids is at least 12,000 years, based on the comparison of our theoretical results compared to the decadal survey of the daytime Arietids meteor shower by CMOR, in particular the spread in nodal longitudes. Finally, our results indicate that P/1999 J6 and perhaps other members of the Marsden group of sunskirters may contribute to the peak of stream but are not able to explain the older “wings”. Hence, these sunskirters alone are not responsible for the stream.

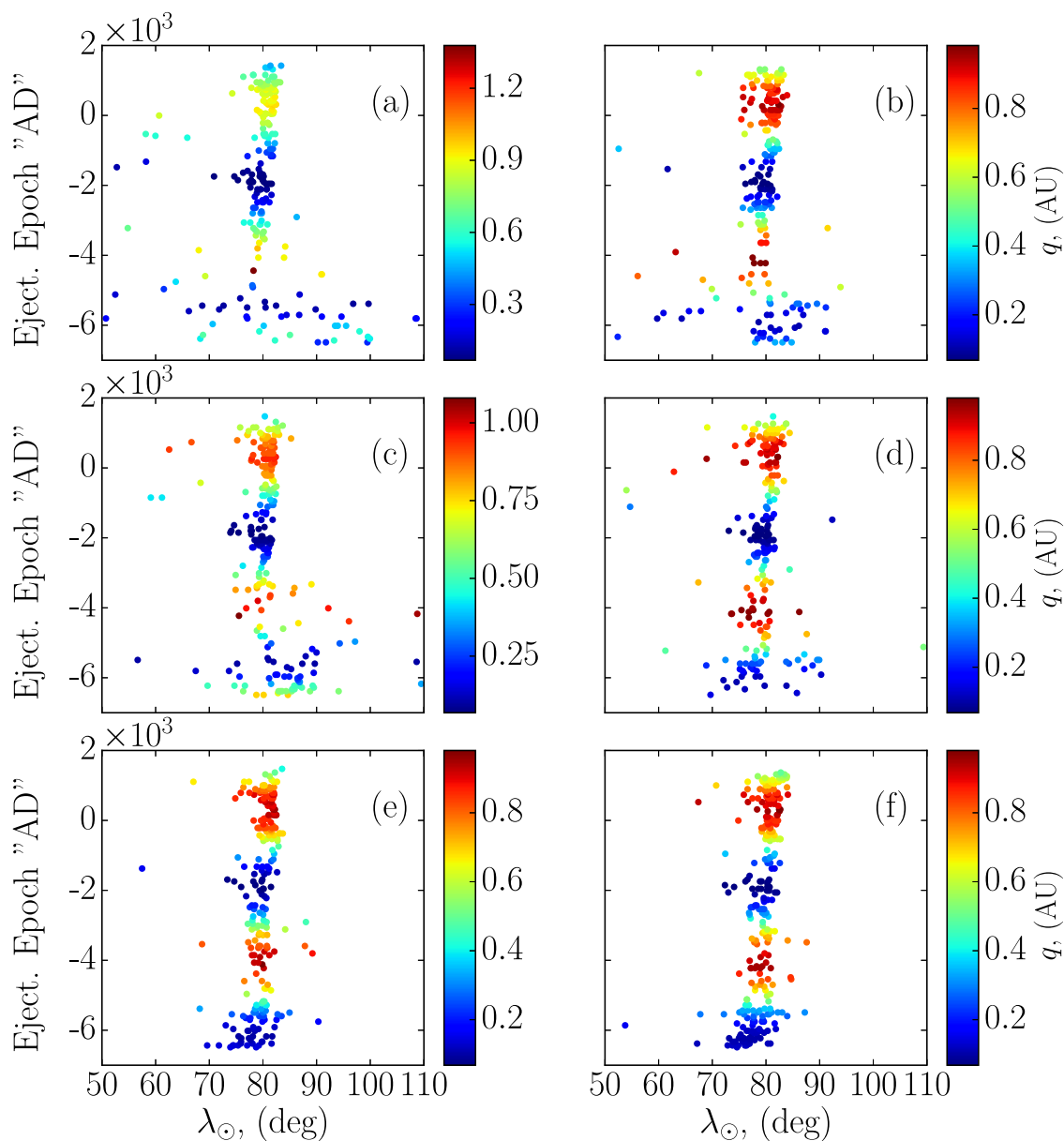


Fig. 20. The present distribution of the solar longitude λ_{\odot} of meteoroids, as a function of the ejection epoch for meteoroid ejection from 96P (case 5) in Table 2. Details as in Fig. 7.

4.2.3. Cases 8 and 9: discrepancy between radar and optical arietids surveys

In previous sections, we briefly discussed the observed discrepancy between some of the orbital elements of the Arietids as deduced from radar and optical surveys. To address this question more fully, we performed additional simulations (cases 8 and 9 in Table 2 in Section 3.4.3) in order to test whether the inconsistency between the orbital elements of $s = 50 \mu\text{m}$ and millimeter size meteoroids can be attributed to the Poynting–Robertson drag, acting over a prolonged time scale. We first show the results for an assumed age of 30000 BC (case 9) and we then compare these results to case 8 (20000 BC).

Fig. 24 shows the simulated distribution of the orbital elements for the daytime Arietids, ejected from one particular clone of 96P/Machholz in 30,000 BC (case 9). It is evident from the figure that the action of Poynting–Robertson drag, over a time interval of 32,000 years, is sufficient to decrease the semi-major axis of $50 \mu\text{m}$ size Arietids, to their presently observed values by CMOR, though

the nodal timing for these meteoroids is inconsistent with the observations. That is, meteoroids with semi-major axis of the order of 1.5 AU and below, would peak a month later than the presently observed time of maximum activity, for our particular starting orbits. Moreover, it is also evident from Fig. 24 that the continuous action of the Poynting–Robertson drag, over 32,000 years, decreases the eccentricity of meteoroids' orbits to values as low as $e \approx 0.88$, whereas CMOR yields values of the order of $e \approx 0.96$. An obvious discrepancy is also observed between the angular orbital elements (inclination and argument of perihelion), as well as the perihelion and aphelion distances, with other clones of 96P/Machholz yielding similar results. This is not surprising as we are using test orbits for the stream, much older than it is possible to know the true parent and hence the simulated particles end up in random phases of the Kozai cycle.

The simulated radiant positions of individual Arietids, ejected in 30,000 BC (case 9) is presented in Fig. 25. Evidently, our simulations of the radiant position do not match the radar observations,

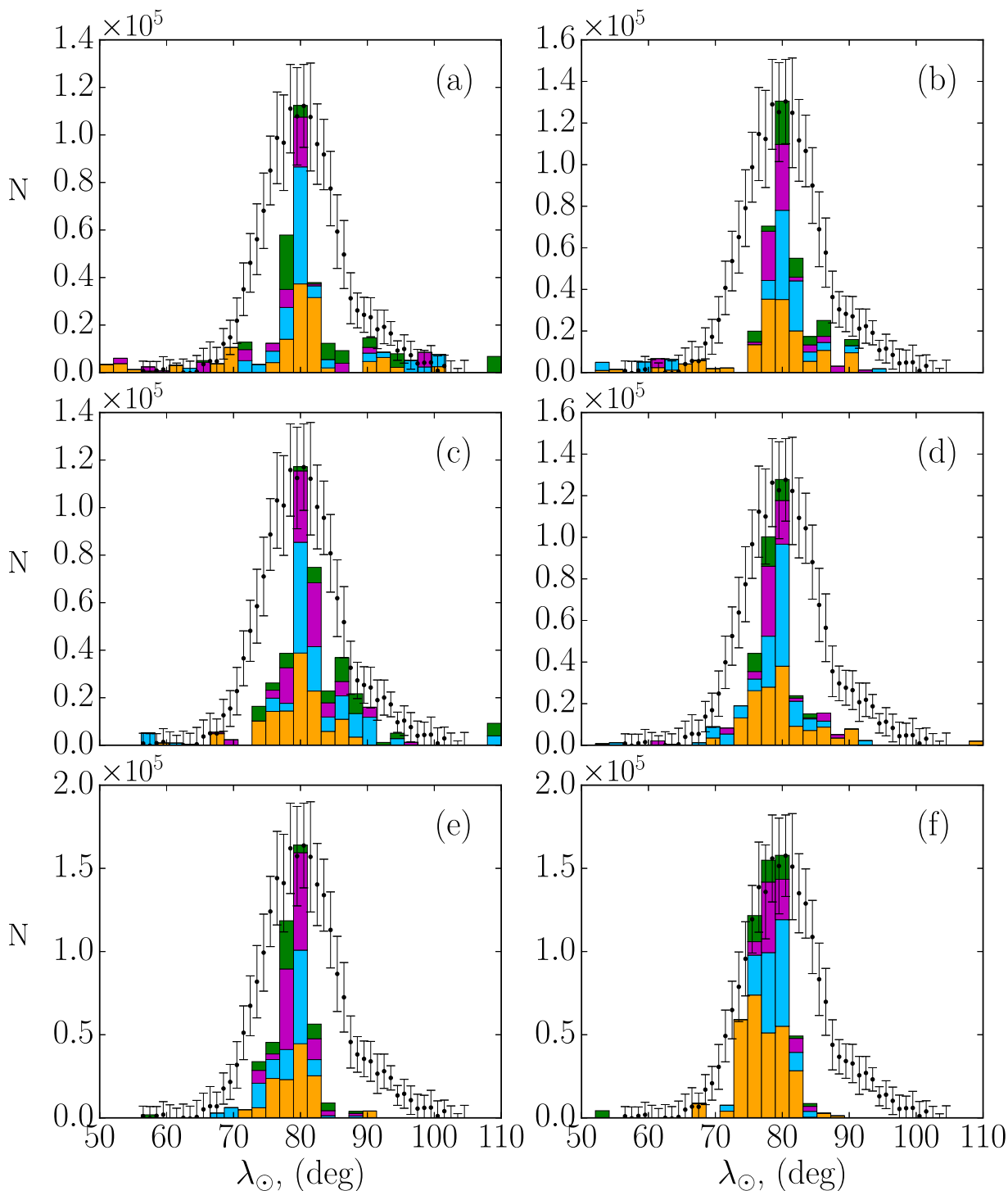


Fig. 21. The weighted activity profile for the daytime Arietids, at the present for meteoroid ejection from comet 96P for case 5. Details as in Fig. 8.

with the simulated radiant positions yielding slightly higher values for the ecliptic latitude of the radiant with a significant scatter in the ecliptic longitude. Clearly, the action of the Poynting–Robertson drag over 32,000 years leads to low values of the semi-major axis and in particular of the eccentricity, where the latter is even significantly lower than the predicted values by CMOR. Without knowing the actual parent orbit this far in the past, we can only say that it is possible that the differential Poynting–Robertson drag has produced the differences in the orbital elements between

the radar and optical measurements and if so, the stream must be much older than $\approx 12,000$ years.

To test whether given a shorter action time scale of the Poynting–Robertson drag can reproduce the observed distribution of the orbital elements of radar Arietids, we ejected 5×10^4 meteoroids from 10 clones of 96P/Machholz in 20,000 BC which is our case 8. We used radius of $s = 50 \mu\text{m}$ for radar sized Arietids, almost certainly a factor of several too small relative to CMOR values. Fig. 26 shows the simulated distribution of the orbital

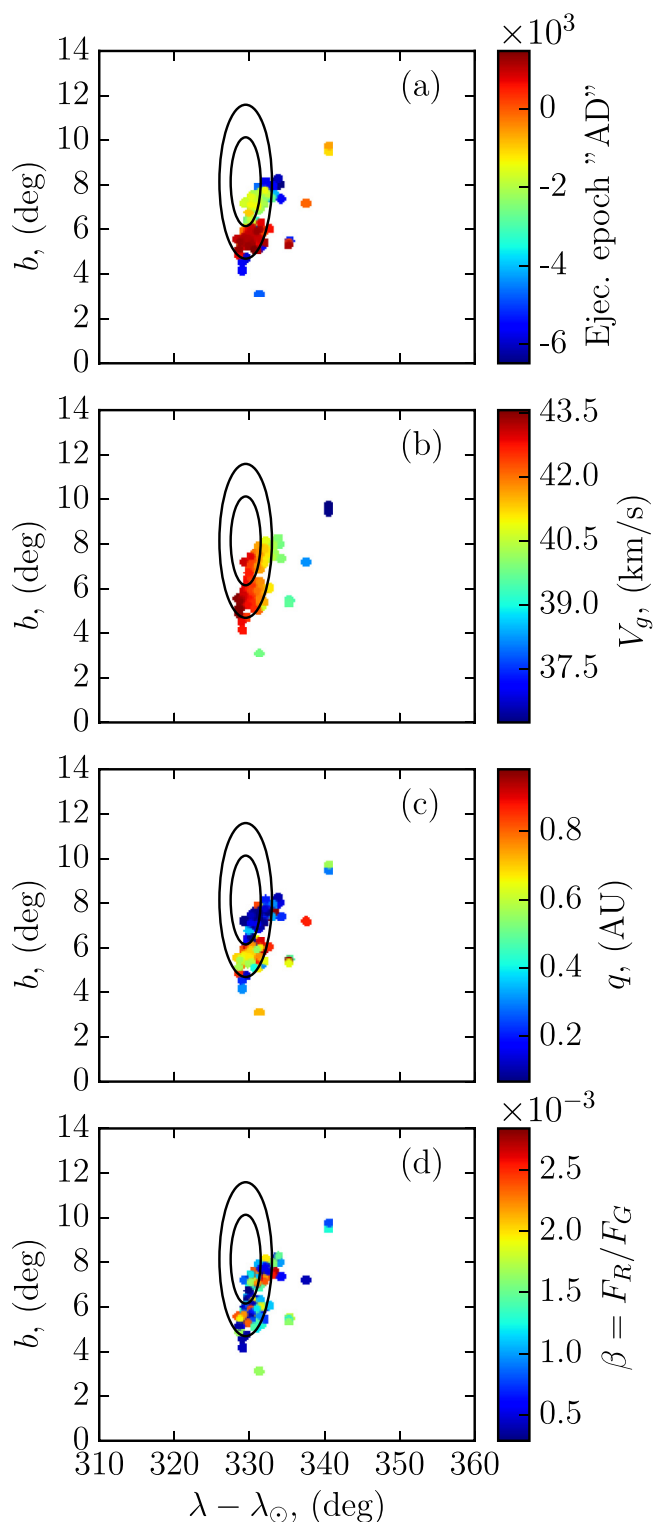


Fig. 22. Radiant position of the simulated daytime Arietids (color dots) for case 5 in Table 2 for clone (b) of comet 96P. Details are as in Fig. 9.

elements of the meteoroids, presently approaching the Earth within 0.01 AU, compared with the radar and optical observations. Although the resulting values of the semi-major axis and eccentricity of the orbits were slightly higher compared to meteoroids ejected in 30,000 BC, the position of the simulated peak activity was again shifted to higher values of solar longitude, predicting that the maximum activity would occur somewhat 30 days later

than the presently observed location of the peak, a situation also observed in case 9. In addition, the angular orbital elements as well as the perihelion and aphelion distances did not fit the observations as expected. Fig. 27 shows the simulated individual radiant positions of the meteoroids for case 8 (20,000 BC). Similar to case 9, the ecliptic latitude was inconsistent with the observations, though the dispersion in the ecliptic longitude was lower compared to meteoroids ejected in 30,000 BC. The rest of the clones yielded similar overall results, with some meteoroids attaining orbits with very low semi-major axis (even lower than the predicted values by CMOR) though the timing (location of the peak) is inconsistent with the observations.

Finally, our simulations suggest that if the daytime Arietids originated from 96P/Machholz, the secular action of Poynting–Robertson drag over a time scale of $(2-3) \times 10^4$ years can significantly decrease the orbits of particles with radii $s = 50 \mu\text{m}$ to values presently observed by radar surveys, though we do not know the true orbit of the parent this far back in the past. This renders it difficult to draw any rigorous conclusions as to the orbit discrepancies between radar and optical daytime Arietid surveys. Furthermore, particles with radii $s = 50 \mu\text{m}$, entering the Earth's atmosphere with geocentric speeds of $V_g \approx 40 \text{ km/s}$ are probably below the detectability threshold of CMOR, given the uncertainties in the mass scale (e.g., Weryk and Brown, 2013).

Unfortunately, we do not presently have sufficient information to argue conclusively as to whether the discrepancy in the orbital elements between radar and optical sized daytime Arietids is due to some systematic errors in radar surveys (e.g., inappropriate account for atmospheric deceleration) or systematic effects in the optical detection of the stream (e.g., all optical detections occur with very low local radiants) or some physical effect which mass separates them on orbits presently detected by radar systems.

5. Discussion and conclusions

We have performed a numerical study to investigate the origin and formation of the daytime Arietids, in order to constrain its age and to investigate the child-parent relationship of the stream with the two proposed parents, comet 96P/Machholz and the Marsden group of sun-skirting comets. Throughout, this work we examined various possible scenarios of the formation of the stream, considering various formation epochs but constraining ourselves to only formation of the stream via normal cometary activity.

We first investigated a possible origin of the daytime Arietids from the Marsden sunskirting group of comets. We considered the most prominent member, namely P/1999 J6 which has survived at least a few perihelion returns to the Sun on an orbit with extreme perihelion distance of $\approx 10 R_\odot$. Our selection of P/1999 J6 was motivated by the fact that most of the Marsden group of sunskirters are very faint and with poorly constrained orbits, while the orbit of P/1999 J6 is relatively reliable. We therefore, tested a possible origin of the stream from P/1999 J6, considering various meteoroid ejection onset epochs (cases 1 through 5, Table 1) as suggested by Sekanina and Chodas (2005). The theoretical characteristics of the resulting stream were compared against the decadal survey of the daytime Arietids by CMOR (Bruzzone et al., 2015).

For case 1, we expected the widest profile, due to earlier ejection times, but case 1 along with all other cases resulted in a very sharp peak of both, the unweighted and weighted activity profiles, matching the observed location of the maximum activity, though producing a very narrow overall profile, inconsistent with the observations by CMOR. As a result, we conclude P/1999 J6 cannot have produced the entire Arietids stream though it may well contribute to its core. The theoretical distribution of many of the orbital elements such as, the semi-major axis a , eccentricity e and aphelion distance Q , as a function of the solar longitude λ_\odot , do

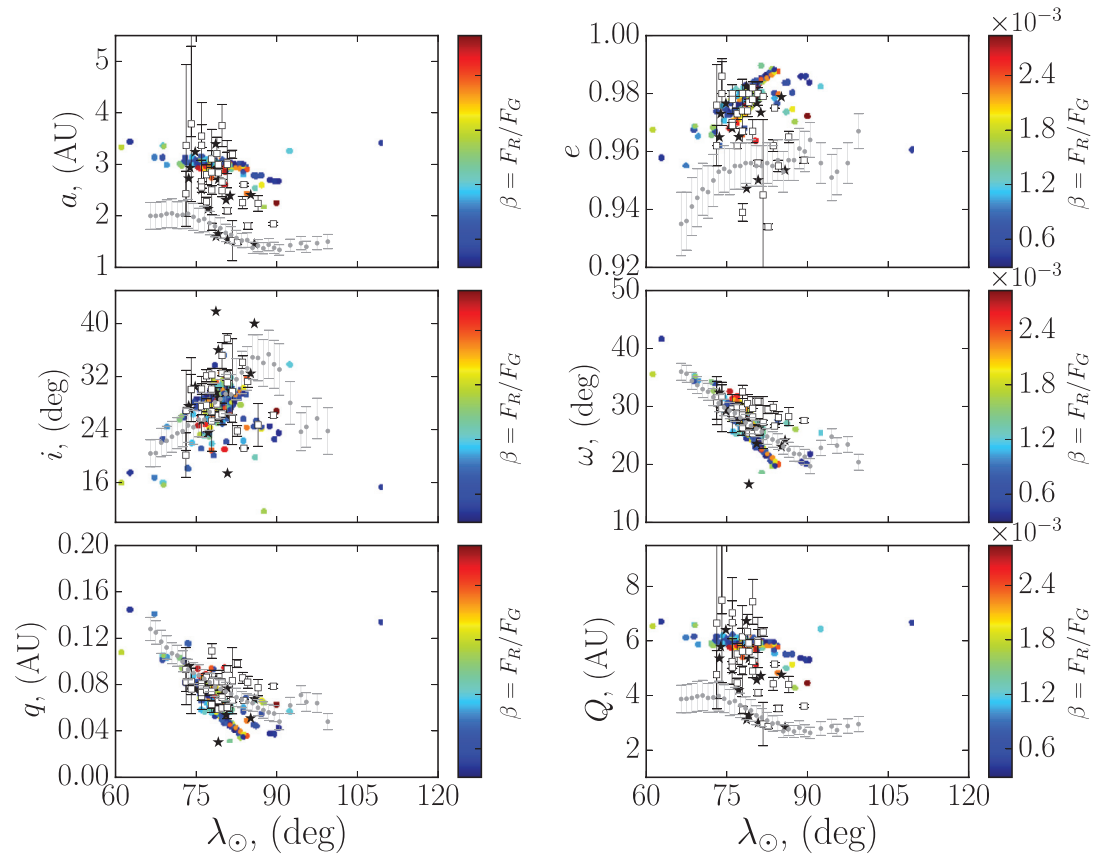


Fig. 23. Distribution of the mean orbital elements of meteoroids ejected from 96P, for case 5. See Fig. 10 for details.

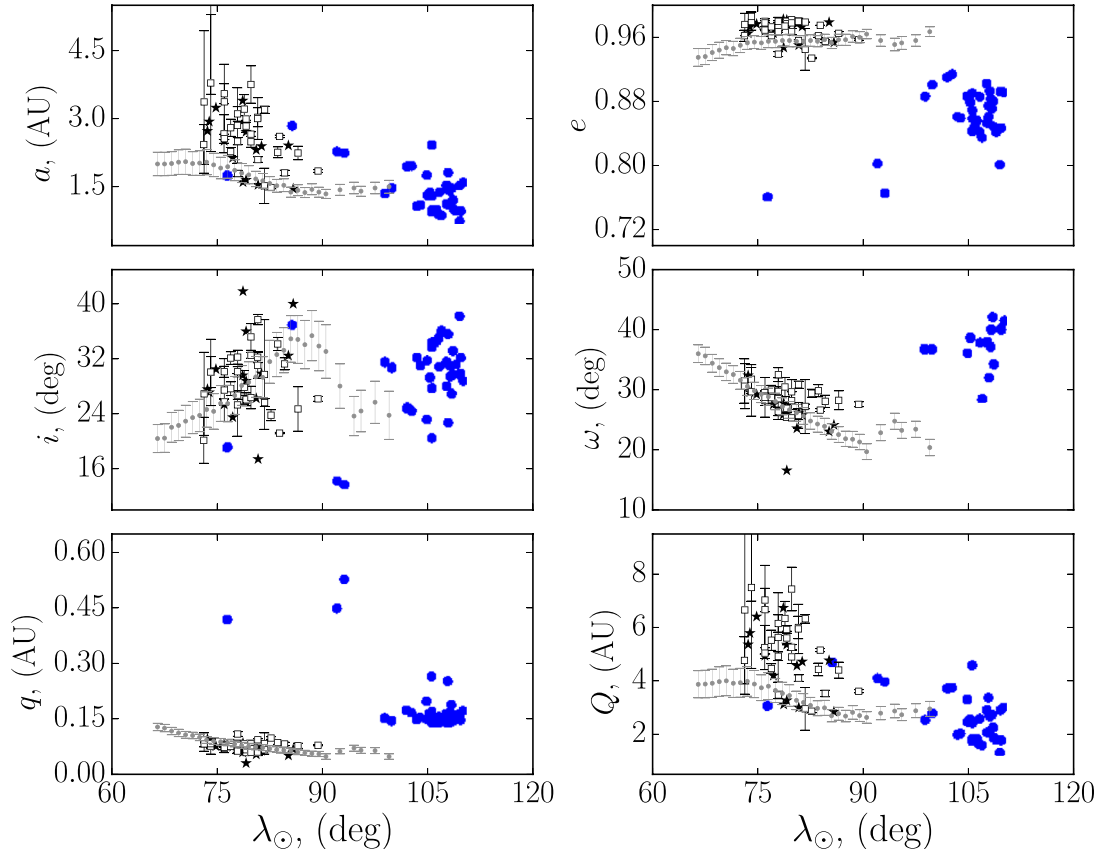


Fig. 24. Distribution of the mean orbital elements of simulated daytime Arietids (blue dots) with radii $s = 50 \mu\text{m}$, ejected in 30000 BC (case 9) from one particular clone of 96P. The observations by various meteor surveys are superimposed (see Fig. 10). (For interpretation of the references to colour in this figure legend, the reader is referred to the web version of this article.)

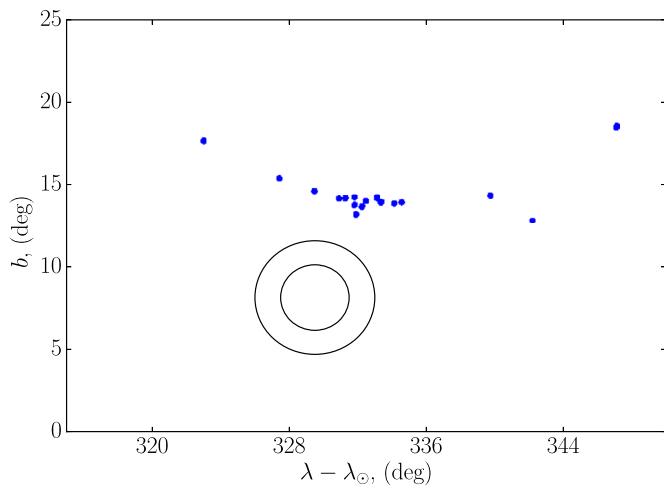


Fig. 25. Individual radiant position distribution (blue dots) for meteoroids of size $s = 50 \mu\text{m}$, ejected in 30000 BC (case 9) from one particular clone of comet 96P. The two superimposed circles correspond to 68% and 95% confidence regions of the mean radiant of the Arietids, as derived by CMOR (Bruzzone et al., 2015). (For interpretation of the references to colour in this figure legend, the reader is referred to the web version of this article.)

not match the radar observations, where the numerical integrations yield systematically higher values for a , e and Q , mostly consistent with optical surveys of the daytime Arietids by SonotaCo and CAMS.

For the second parent candidate, 96P/Machholz, we investigated nine different scenarios (cases 1 through 9, Table 2) assuming various meteoroid ejection onset times and variable dust production rate for some cases. Similar to the case with P/1999 J6 (above), we utilized a weighting factor as a function of the parent body's perihelion distance at the time of ejection.

The best match between the observed and simulated characteristics of the daytime Arietids, assuming an origin from 96P/Machholz, was observed for case 7, with an onset 12,000 years ago and a decreasing dust production over time through the present. For this simulation, the match in the activity profiles was very good, with the model being able to reproduce both the location of the peak and the width of the observed activity profile. Other cases produced a good fit to the location of the peak, though the width of the profile was too narrow and thus inconsistent with the observations by CMOR. The radiant location was a good match for all cases with the bulk of the individual radiants being within the 95% confidence region of the mean radiant position as deduced by CMOR. Similar to the case with P/1999 J6, there was a correlation between the individual radiant location and the particles' geocentric speed, with slower particles having radiant outside the 95% confidence region of the observed radiant, so those slow particles might not have been counted as Arietids by CMOR's software.

Despite the very good match of the activity profile and radiant position for case 7, there was still a discrepancy between the observed radar and simulated distribution of orbital elements of the meteoroids as a function of the solar longitude. Our simulations

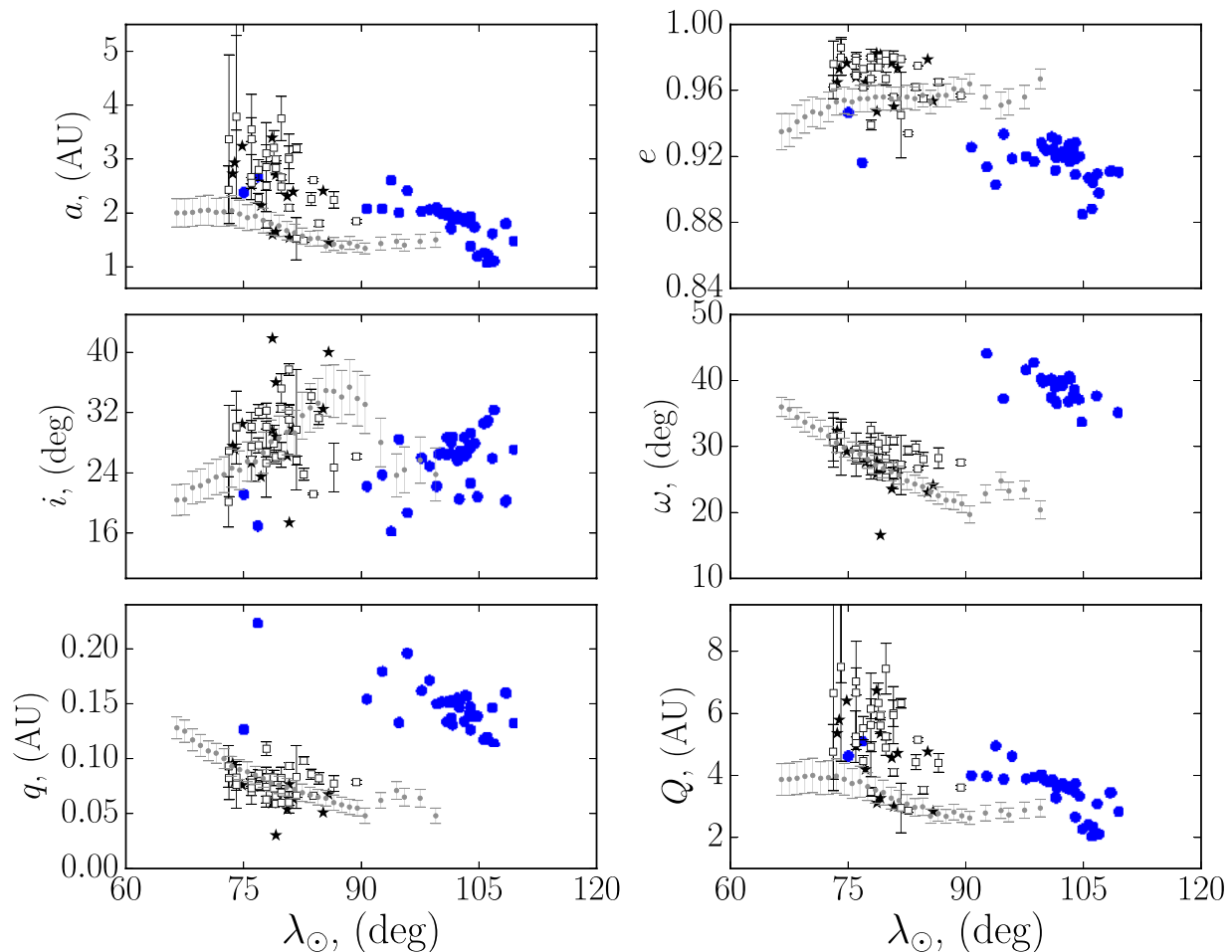


Fig. 26. Distribution of the mean orbital elements of simulated daytime Arietids (blue dots) with radii $s = 50 \mu\text{m}$, ejected in 20000 BC (case 8) from one particular clone of 96P. The observations by various meteor surveys are superimposed (see Fig. 10). (For interpretation of the references to colour in this figure legend, the reader is referred to the web version of this article.)

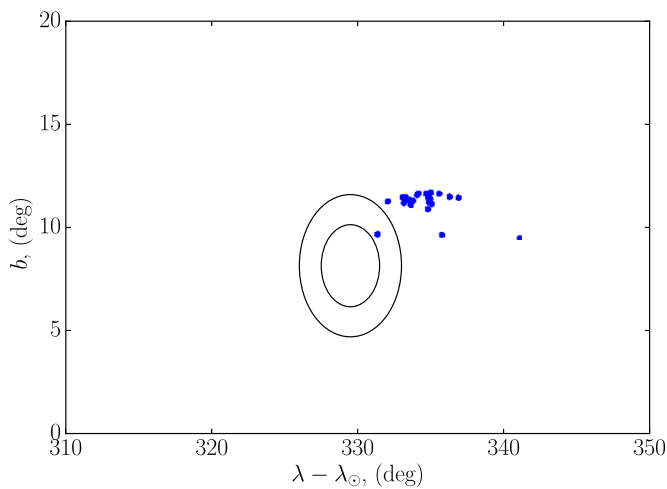


Fig. 27. Individual radiant position distribution (blue dots) for meteoroids of size $s = 50 \mu\text{m}$, ejected in 20000 BC (case 8) from one particular clone of comet 96P. The two superimposed circles correspond to 68% and 95% confidence regions of the mean radiant of the Arietids, as derived by CMOR (Bruzzone et al., 2015). (For interpretation of the references to colour in this figure legend, the reader is referred to the web version of this article.)

yielded systematically higher values for the semi-major axis a , eccentricity e and the aphelion distance Q than the radar data, but consistent with optical surveys of the daytime Arietids by SonotaCo (SonotaCo, 2009) and CAMS Jenniskens et al. (2016).

Lastly, we utilized cases 8 and 9 to investigate if the discrepancy in the orbital elements as deduced from radar and optical surveys can be attributed solely to the Poynting–Robertson drag, acting on radar size particles. We investigated two different cases with particles of radii $s = 50 \mu\text{m}$ released from 96P/Machholz at two different discrete eras, 20,000 BC and 30,000 BC. These time scales are comparable to the dynamical lifetime of short-period comets 4.5×10^4 (Levison and Duncan, 1994), thus rendering meteoroid stream investigations beyond that time, problematic. Moreover, it is doubtful that 96P could survive 30,000 years in an orbit that periodically brings it at a sungrazing state. This is further motivated that these time scales exceed the physical life time of JFCs, which has a median value of 12,000 years (Levison and Duncan, 1997).

We conclude that the continuous action of Poynting–Robertson drag, over time scales of $(2\text{--}3) \times 10^4$ years may decrease the semi-major axis to the presently observed values by radar surveys, though the location of the peak was inconsistent, being more than a month later than its present value. We note the choice of particles with radii $s = 50 \mu\text{m}$, hitting the Earth’s atmosphere, are extreme lower limits to the detection of the daytime Arietids by CMOR, rendering the obtained values for the semi-major axis of the orbits only a lower limit.

In summary, we conclude that the daytime Arietid meteoroid stream is most likely associated with comet 96P/Machholz and has an age of at least 12,000 years. However, a child-parent relationship between the Arietids and the Marsden group of sun-skirting comets can not be completely ruled out, and P/1999 J6 may contribute to the core of the stream. Unfortunately, we can not discern whether the discrepancy between the orbital elements, derived from radar and optical surveys, is real or an artifact. However, our simulations suggest that if the mass segregation is real, then the stream must be several tens of thousands of years old, in order for such a large difference between the orbital elements to exist.

Acknowledgements

Funding from the NASA Meteoroid Environment office through NASA co-operative agreement NNX15AC94A is gratefully acknowledged. Funding for this work was also received from the Natural Sciences and Engineering Research Program and the Canada Research Chairs program. We also thank the reviewers, Dr. David Asher and Dr. Jeremie Vaubaillon, for their useful comments and suggestions for improving this work.

References

- A’Hearn, M.F., Millis, R.C., Schleicher, D.O., Osip, D.J., Birch, P.V., 1995. The ensemble properties of comets: results from narrowband photometry of 85 comets, 1976–1992. *Icarus* 118, 223–270. doi:10.1006/icar.1995.1190.
- Almond, M., 1951. The summer daytime meteor streams of 1949 and 1950. III. Computation of the orbits. *MNRAS* 111, 37.
- Aspinall, A., Clegg, J.A., Lovell, A.C.B., 1949. The daytime meteor streams of 1948. Part I. Measurement of the Activity and radiant positions. *MNRAS* 109, 352.
- Aspinall, A., Hawkins, G.S., 1951. The summer daytime meteor streams of 1949 and 1950. I. Measurement of the radiant positions and activity. *MNRAS* 111, 18.
- Babadzhanov, P.B., Kokhirova, G.I., 2009. Densities and porosities of meteoroids. *A&A* 495, 353–358. doi:10.1051/0004-6361/200810460.
- Babadzhanov, P.B., Obrubov, Y.V., 1992. P/Machholz 1986 VIII and quadrantid meteoroid stream. Orbital evolution and relationship. In: Harris, A.W., Bowell, E. (Eds.), *Asteroids, Comets, Meteors 1991*, pp. 27–32.
- Babadzhanov, P.B., Obrubov, Y.V., 1993. Dynamics and relationship between interplanetary bodies: comet P/Machholz and its meteor showers. In: Stohl, J., Williams, I.P. (Eds.), *Meteoroids and their Parent Bodies*, p. 49.
- Baggaley, W.J., Bennett, R.G.T., Steel, D.I., Taylor, A.D., 1994. The advanced meteor orbit radar facility - AMOR. *Q. J. R. Astron. Soc.* 35, 293.
- Bailey, M.E., Chambers, J.E., Hahn, G., 1992. Origin of sungrazers - A frequent cometary end-state. *A&A* 257, 315–322.
- Brasser, R., Wiegert, P., 2008. Asteroids on Earth-like orbits and their origin. *MNRAS* 386, 2031–2038. doi:10.1111/j.1365-2966.2008.13146.x.
- Brown, P., Jones, J., 1998. Simulation of the formation and evolution of the perseid meteoroid stream. *Icarus* 133, 36–68. doi:10.1006/icar.1998.5920.
- Bruzzone, J.S., Brown, P., Weryk, R.J., Campbell-Brown, M.D., 2015. A decadal survey of the daytime arietid meteor shower using the Canadian meteor orbit radar. *MNRAS* 446, 1625–1640. doi:10.1093/mnras/stu2200.
- Burns, J.A., Lamy, P.L., Soter, S., 1979. Radiation forces on small particles in the solar system. *Icarus* 40, 1–48. doi:10.1016/0019-1035(79)90050-2.
- Campbell-Brown, M.D., 2004. Radar observations of the arietids. *MNRAS* 352, 1421–1425. doi:10.1111/j.1365-2966.2004.08039.x.
- Carusi, A., Kresak, L., Perozzi, E., Valsecchi, G.B., 1987. High-order librations of Halley-type comets. *A&A* 187, 899.
- Chambers, J.E., 1999. A hybrid symplectic integrator that permits close encounters between massive bodies 304, 793–799.
- Clegg, J.A., Hughes, V.A., Lovell, A.C.B., 1947. The daylight meteor streams of 1947 May–August. *MNRAS* 107, 369.
- Davies, J.G., Greenhow, J.S., 1951. The summer daytime meteor streams of 1949 and 1950. II. Measurement of the velocities. *MNRAS* 111, 26.
- Delsemme, A.H., 1982. Chemical composition of cometary nuclei. In: Wilkening, L.L. (Ed.), *IAU Colloq. 61: Comet Discoveries, Statistics, and Observational Selection*, pp. 85–130.
- Fujiwara, Y., Ueda, M., Sugimoto, M., Sagayama, T., Abe, S., 2004. TV observation of the daytime meteor shower; the arietids. *Earth Moon Planets* 95, 595–600. doi:10.1007/s11038-005-5040-2.
- Hawkes, R.L., 1993. Television meteors (Invited). In: Stohl, J., Williams, I.P. (Eds.), *Meteoroids and their Parent Bodies*, p. 227.
- Hawkes, R.L., 2002. Meteors in the Earth’s Atmosphere. p. 97.
- Jakubík, M., Neslušan, L., 2015. Meteor complex of asteroid 3200 Phaethon: its features derived from theory and updated meteor data bases. *MNRAS* 453, 1186–1200. doi:10.1093/mnras/stv1643.
- Jenniskens, P., Duckworth, H., Grigsby, B., 2012. Daytime Arietids and Marsden Sun-skirters (ARI, IAU #171). *WGN, J. Int. Meteor. Org.* 40, 98–100.
- Jenniskens, P., Gural, P.S., Dynneson, L., Grigsby, B.J., Newman, K.E., Borden, M., Koop, M., Holman, D., 2011. CAMS: Cameras for Allsky Meteor Surveillance to establish minor meteor showers. *Icarus* 216, 40–61. doi:10.1016/j.icarus.2011.08.012.
- Jenniskens, P., Nénon, Q., Albers, J., Gural, P.S., Haberman, B., Holman, D., Morales, R., Grigsby, B.J., Samuels, D., Johannink, C., 2016. The established meteor showers as observed by CAMS. *Icarus* 266, 331–354. doi:10.1016/j.icarus.2015.09.013.
- Jenniskens, P., Vaubaillon, J., 2007. 3D/Biela and the Andromedids: fragmenting versus sublimating comets. *Astron. J.* 134, 1037–1045. doi:10.1086/519074.
- Jenniskens, P., Vaubaillon, J., 2010. Minor planet 2002 EX₁₂ (=1969P/NEAT) and the alpha Capricornid shower. *Astron. J.* 139, 1822–1830. doi:10.1088/0004-6256/139/5/1822.
- Jones, J., 2003. Modeling the sporadic meteoroid complex. Cooperative agreement NCC8-185 between University of Western Ontario and NASA 1–51.
- Jones, J., Brown, P., Ellis, K.J., Webster, A.R., Campbell-Brown, M., Krzeminski, Z., Weryk, R.J., 2005. The Canadian meteor orbit radar: system overview and preliminary results. *Planet. Space Sci.* 53, 413–421. doi:10.1016/j.pss.2004.11.002.

- Jones, J., Jones, W., 1993. Comet Machholz and the Quadrantid meteor stream. *MNRAS* 261, 605–611.
- Kinoshita, H., Nakai, H., 1999. Analytical solution of the Kozai resonance and its application. *Celestial Mech. Dyn. Astron.* 75, 125–147. doi:10.1023/A:1008321310187.
- Klačka, J., 2004. Electromagnetic radiation and motion of a particle. *Celestial Mech. Dyn. Astron.* 89, 1–61. doi:10.1023/B:CELE.0000028165.34272.d9.astro-ph/0301138.
- Kozai, Y., 1962. Secular perturbations of asteroids with high inclination and eccentricity. *Astron. J.* 67, 591. doi:10.1086/108790.
- Kresak, L., 1976. Orbital evolution of the dust streams released from comets. *Bull. Astron. Inst. Czechoslovakia* 27, 35–46.
- Langland-Shula, L.E., Smith, G.H., 2007. The unusual Spectrum of comet 96P/Machholz. *ApJ* 664, L119–L122. doi:10.1086/520839. 0706.2022.
- Leinert, C., Grun, E., 1990. Interplanetary dust. p. 207.
- Levison, H.F., Duncan, M.J., 1994. The long-term dynamical behavior of short-period comets. *Icarus* 108, 18–36. doi:10.1006/icar.1994.1039.
- Levison, H.F., Duncan, M.J., 1997. From the Kuiper belt to Jupiter-family comets: the spatial distribution of ecliptic comets. *Icarus* 127, 13–32. doi:10.1006/icar.1996.5637.
- McIntosh, B.A., 1990. Comet P/Machholz and the Quadrantid meteor stream. *Icarus* 86, 299–304. doi:10.1016/0019-1035(90)90219-Y.
- McKinley, D. W. R., 1961. Meteor science and engineering.
- Murray, C.D., Dermott, S.F., 2000. *Solar system dynamics*.
- Neslušan, L., Hajduková, M., 2014. The meteor-shower complex of comet C/1917 F1 (Mellish). *A&A* 566, A33. doi:10.1051/0004-6361/201423382.
- Neslušan, L., Kaňuchová, Z., Tomko, D., 2013. The meteor-shower complex of 96P/Machholz revisited. *A&A* 551, A87. doi:10.1051/0004-6361/201220299.
- Ohtsuka, K., Nakano, S., Yoshikawa, M., 2003. On the Association among Periodic Comet 96P/Machholz, Arietids, the Marsden Comet Group, and the Kracht Comet Group. *Publ. Astr. Soc. Japan* 55, 321–324. doi:10.1093/pasj/55.1.321.
- Peterson, A.W., 1971. A determination of the vaporization temperature of circum-solar dust at 4 R sun. In: *Bulletin of the American Astronomical Society*. In: *Bulletin of the American Astronomical Society*, vol. 3, p. 500.
- Rickman, H., Fernandez, J.A., Gustafson, B.A.S., 1990. Formation of stable dust mantles on short-period comet nuclei. *A&A* 237, 524–535.
- Robertson, H.P., 1937. Dynamical effects of radiation in the solar system. *MNRAS* 97, 423. doi:10.1093/mnras/97.6.423.
- Schleicher, D.G., 2008. The extremely anomalous molecular abundances of comet 96P/Machholz 1 from Narrowband photometry. *Astron. J.* 136, 2204–2213. doi:10.1088/0004-6256/136/5/2204.
- Sekanina, Z., 1977. Relative motions of fragments of the split comets. I - A new approach. *Icarus* 30, 574–594. doi:10.1016/0019-1035(77)90111-7.
- Sekanina, Z., 1978. Relative motions of fragments of the split comets. II - Separation velocities and differential decelerations for extensively observed comets. *Icarus* 33, 173–185. doi:10.1016/0019-1035(78)90031-3.
- Sekanina, Z., 2005. Comet 73P/Schwassmann–Wachmann: Nucleus Fragmentation, Its Light-Curve Signature, and Close Approach to Earth in 2006. *Int. Comet Q.* 27, 225–240.
- Sekanina, Z., Chodas, P.W., 2005. Origin of the Marsden and Kracht Groups of Sunskirting Comets. I. Association with Comet 96P/Machholz and Its Interplanetary Complex. *ApJS* 161, 551–586. doi:10.1086/497374.
- SonotaCo, 2009. A meteor shower catalog based on video observations in 2007–2008. *WGN, J. Int. Meteor Org.* 37, 55–62.
- Vaubailon, J., Lamy, P., Jorda, L., 2006. On the mechanisms leading to orphan meteoroid streams. *MNRAS* 370, 1841–1848. doi:10.1111/j.1365-2966.2006.10606.x.
- Weryk, R.J., Brown, P.G., 2013. Simultaneous radar and video meteors II: photometry and ionisation. *Planet. Space Sci.* 81, 32–47. doi:10.1016/j.pss.2013.03.012.
- Whipple, F.L., 1950. A comet model. I. The acceleration of Comet Encke. *ApJ* 111, 375–394. doi:10.1086/145272.
- Whipple, F.L., 1951. A Comet Model. II. Physical relations for Comets and Meteors.. *ApJ* 113, 464. doi:10.1086/145416.
- Wiegert, P., Brown, P., 2005. The quadrantid meteoroid complex. *Icarus* 179, 139–157. doi:10.1016/j.icarus.2005.05.019.
- Williams, I.P., 1992. The dynamics of meteoroid streams (lecture). In: Ferraz-Mello, S. (Ed.), *Chaos, Resonance, and Collective Dynamical Phenomena in the Solar System*. IAU Symposium, vol. 152, p. 299.